AD NUMBER

ADB016529

LIMITATION CHANGES

TO:

Approved for public release; distribution is unlimited.

FROM:

Distribution authorized to U.S. Gov't. agencies only; Test and Evaluation; FEB 1977. Other requests shall be referred to Air Force Flight Dynamics Lab., Wright-Patterson AFB, OH 45433.

AUTHORITY

AFWAL ltr 6 Nov 1980

AEDC-TR-77-7

AERODYNAMIC AND THERMAL PERFORMANCE CHARACTERISTICS OF SUPERSONIC-X TYPE DECELERATORS AT MACH NUMBER 8

VON KARMAN GAS DYNAMICS FACILITY
ARNOLD ENGINEERING DEVELOPMENT CENTER
AIR FORCE SYSTEMS COMMAND
ARNOLD AIR FORCE STATION, TENNESSEE 37389

This document has been approved for public release
its distribution is unlimited. February 1977

Final Report for Period August 4 — 9, 1976

Distribution limited to U. S. Government agencies only; this report contains information on test and evaluation of military hardware; February 1977; other requests for this document must be referred to Air Force Flight Dynamics Laboratory (AFFDL/FER), Wright-Patterson AFB, OH 45433.

Prepared for

AIR FORCE FLIGHT DYNAMICS LABORATORY (AFFDL/FER)
WRIGHT-PATTERSON AIR FORCE BASE, OHIO 45433

NOTICES

When U. S. Government drawings specifications, or other data are used for any purpose other than a definitely related Government procurement operation, the Government thereby incurs no responsibility nor any obligation whatsoever, and the fact that the Government may have formulated, furnished, or in any way supplied the said drawings, specifications, or other data, is not to be regarded by implication or otherwise, or in any manner licensing the holder or any other person or corporation, or conveying any rights or permission to manufacture, use, or sell any patented invention that may in any way be related thereto.

Qualified users may obtain copies of this report from the Defense Documentation Center.

References to named commercial products in this report are not to be considered in any sense as an endorsement of the product by the United States Air Force or the Government.

APPROVAL STATEMENT

This technical report has been reviewed and is approved for publication.

FOR THE COMMANDER

Chauncey D. Smith, Jr.

CHAUNCEY D. SMITH, JR.
Lt Colonel, USAF
Chief Air Force Test Director, VKF
Directorate of Test

Alan L. Devereaux

ALAN L. DEVEREAUX
Colonel, USAF
Director of Test

REPORT DOCUMENTATION PAGE		READ INSTRUCTIONS BEFORE COMPLETING FORM
1 REPORT NUMBER AEDC-TR-77-7	2 GOVT ACCESSION NO.	3 RECIPIENT'S CATALOG NUMBER
4 TITLE (and Subtitle) AERODYNAMIC AND THERMAL PERFORMANCE CHARACTERISTICS OF SUPERSONIC-X TYPE DECELERATORS AT MACH NUMBER 8		5 TYPE OF REPORT & PERIOD COVERED Final Report - August 4-9, 1976 6 PERFORMING ORG. REPORT NUMBER
7 AUTHOR(s) J. D. Corce, ARO, Inc.		8 CONTRACT OR GRANT NUMBER(s)
9 PERFORMING ORGANIZATION NAME AND ADDRESS Arnold Engineering Development Center (XO) Air Force Systems Command Arnold Air Force Station, Tennessee 37389		10. PROGRAM ELEMENT, PROJECT, TASK AREA & WORK UNIT NUMBERS Program Element 62201F, Project 6065, Task 01
11 CONTROLLING OFFICE NAME AND ADDRESS Air Force Flight Dynamics Laboratory (AFFDL/FER) Wright-Patterson Air Force Base, Ohio 45433		12. REPORT DATE February 1977 13 NUMBER OF PAGES 42
14 MONITORING AGENCY NAME & ADDRESS(if different from Controlling Office)		15 SECURITY CLASS. (of this report) UNCLASSIFIED 15a DECLASSIFICATION DOWNGRADING SCHEDULE N/A

16 DISTRIBUTION STATEMENT (of this Report) Distribution limited to U.S. Government agencies only; this report contains information on test and evaluation of military hardware; February 1977; other requests for this document must be referred to Air Force Flight Dynamics Laboratory (AFFDL/FER), Wright-Patterson Air Force Base, Ohio 45433.

17 DISTRIBUTION STATEMENT (of the abstract entered in Block 20, if different from Report)

18 SUPPLEMENTARY NOTES

Available in DDC

19 KEY WORDS (Continue on reverse side if necessary and identify by block number)

parachutes
deceleration
aerodynamic characteristics
thermal properties
hypersonic flow
wind tunnel tests

20 ABSTRACT (Continue on reverse side if necessary and identify by block number)

Wind tunnel test results of the aerodynamic and thermal performance characteristics of model nylon, Kevlar 29, and Bisbenzimidazobenzophenanthroline Supersonic-X type parachutes behind a cone forebody at $M_\infty = 8.0$ are presented. The test was conducted at free-stream unit Reynolds numbers from 1.1 to 3.6 million per foot, simulating pressure altitudes ranging from 145,000 to 130,000 ft, respectively. Drag data are presented which show increased axial force with increasing trailing distance and/or

DD FORM 1 JAN 73 1473 EDITION OF 1 NOV 65 IS OBSOLETE

20. ABSTRACT (Continued)

increasing dynamic pressure. Wake survey pressure and total temperature profiles are presented which show the symmetrical nature of the wake and the effects of the forebody mounting struts.

PREFACE

The work reported herein was conducted by the Arnold Engineering Development Center (AEDC), Air Force Systems Command (AFSC), at the request of the Air Force Flight Dynamics Laboratory (AFFDL/FER) under Program Element 62201F. The monitor for this project was Mr. Charles A. Babish III, AFFDL/FER, Wright-Patterson Air Force Base, Ohio. The results of the test were obtained by ARO, Inc. (a subsidiary of Sverdrup Corporation), contract operator of AEDC, AFSC, Arnold Air Force Station, Tennessee, under ARO Project No. V41B-G2A. The author of this report was J. D. Corce, ARO, Inc. The test was conducted from August 4 to August 9, 1976, and data reduction was completed on September 2, 1976. The manuscript (ARO Control No. ARO-VKF-TR-76-137) was submitted for publication on November 19, 1976.

CONTENTS

ILLUSTRATIONS

TABLE

1.0 INTRODUCTION

Supersonic deployable aerodynamic decelerators, such as Supersonic-X parachutes, operate in the wake of and provide drag and stability for Air Force re-entry and test vehicles, special and conventional weapons, and aircraft crew escape modules that are moving through the atmosphere at supersonic speeds. The aerodynamic and thermal performance characteristics of trailing supersonic decelerators are influenced by the Mach numbers and total temperatures of the forebody wake ahead of the decelerators. These wake flow properties are characterized by Mach numbers from 1.0 to 3.5 and total temperatures from 100 to 700°F.

Results from a previous experimental investigation (Ref. 1) conducted in the von Kármán Gas Dynamics Facility (VKF) Hypersonic Wind Tunnel (B) showed that reasonable approximations of these flow properties could be achieved in the near wake core of a cone forebody immersed in a Mach number 8 free stream at wind tunnel total temperatures of 860 and 1,220°R.

The present test objectives were to determine the aerodynamic and thermal performance characteristics of model nylon, Kevlar 29®, and Bisbenzimidazobenzophenanthroline® (BBB) Supersonic-X type parachutes in four configurations. The decelerators were tested at several axial locations in the wake of a strut-mounted cone forebody. All the configurations were tested at simulated pressure altitudes from 130,000 to 145,000 ft, corresponding to free-stream dynamic pressures from 2 to 1 psia. The free-stream unit Reynolds number was varied from 1.1 to 3.6 million per foot. The investigation was made at wind tunnel stagnation temperatures both above and below that required to prevent air liquefaction in the test section. The lower temperature was required because of the nylon and Kevlar 29 material temperature limits. Wake survey data were obtained at several locations downstream of the forebody to determine local wake conditions, strut effects, and verification of wake survey data obtained in Ref. 1.

Wake survey pitot pressure, static pressure, and total temperature results and selected average drag coefficients of the various configurations showing the effects of location in the wake and free-stream dynamic pressure are presented. Decelerator stability performance is presented in the form of a relative dynamic parameter (RDP).

2.0 APPARATUS

2.1 WIND TUNNEL

Tunnel B is a closed-circuit hypersonic wind tunnel with a 50-in.-diam test section. Two axisymmetric contoured nozzles are available to provide Mach numbers of 6 and 8, and the tunnel may be operated continuously over a range of pressure levels from 20 to 300 psia at M_∞ = 6, and 50 to 900 psia at M_∞ = 8, with air supplied by the VKF main compressor plant. Stagnation temperatures sufficient to avoid air liquefaction in the test section (up to 1,350°R) are obtained through the use of a natural-gas-fired combustion heater. The entire tunnel (throat, nozzle, test section, and diffuser) is cooled by integral, external water jackets. The tunnel is equipped with a model injection system, which allows removal of the model from the test section while the tunnel remains in operation. A description of the tunnel may be found in Ref. 2.

2.2 TEST ARTICLE

The forebody cone support system and a Supersonic-X type parachute are shown installed in the tunnel in Fig. 1 and schematically portrayed in Fig. 2. Two designs of decelerators (designs 2 and 5) were tested with 5- and 8-in. diameters (see Fig. 3) at various X/D locations downstream of the forebody base. Three materials, nylon, Kevlar 19, and Bisbenzimidazobenzophenanthroline (BBB) were investigated. The temperature limits of these materials (the temperature at which only 20 percent of the strength of the material at room temperature is retained) are nylon, 860°R; Kevlar 29, 1,210°R; and BBB, 1,410°R.

The forebody cone and support system for this test entry was the same as that used in an earlier Tunnel B test (see Ref. 1). The forebody was a 10-deg, half-angle cone with a 6-in. base diameter. The decelerators were attached to a six-component moment-type balance mounted in the forebody. Both the balance and the cone support system were water cooled.

A wake survey rake (see Fig. 4) with pitot pressure, cone static pressure, and total temperature probes was used to determine local flow conditions downstream of the cone.

2.3 INSTRUMENTATION AND PRECISION

Tunnel B stilling chamber pressure is measured with a 100- or 1,000-psid transducer referenced to a near vacuum. Based on periodic comparisons with secondary standards, the uncertainty (a bandwidth which includes 95-percent of residuals) of the transducers is estimated to be within ±0.1 percent of reading or ±0.06 psi, whichever is greater, for the 100-psid range, and ±0.1 percent of reading or ±0.5 psi, whichever is greater, for the 1,000-psid range. Stilling chamber temperature measurements are made with Chromel®-Alumel® thermocouples which have an uncertainty of ±(1.5°F + 0.375 percent of reading) based on repeat calibrations.

Model forces and moments were measured with a six-component, moment-type, strain-gage balance (Balance No. 4.06-Y-36-014) supplied and calibrated by VKF. Before the test, static loads in each plane and combined static loads were applied to the balance to simulate the range of loads and center-of-pressure locations anticipated during the test. The following uncertainties represent the bands of 95 percent of the measured residuals, based on differences between the applied loads and the corresponding values calculated from the balance calibration equations included in the final data reduction. The range of check loads applied and the measurement uncertainties follow.

Component	Balance Design Loads	Calibration Load Range	Range Of Check Loads	Measurement Uncertainty
Normal force, lb	± 400	± 300	±15	±0.50
Pitching moment,*in. lb	±1,386	±1,386	±46	±1.00
Side force, lb	± 200	± 150	±15	±0.25
Yawing moment,*in. lb	± 693	± 693	±46	±1.00
Rolling moment, in. lb	± 50	± 50	± 0	±0.24
Axial force, lb	0→50	0→50	0→−50†	±0.16

*About balance forward moment bridge.

†Balance was mounted backwards in forebody cone.

No moment calculations were incorporated in the data reduction since only forces were of interest for this test.

The wake survey temperature measurements were made with a Chromel-Alumel thermocouple probe, with a precision of measurement estimated to be ±0.4 percent of reading. The pitot pressure was measured with a 15-psid transducer, referenced to a near vacuum, which has an estimated precision of measurement of ±0.003 psi or ±0.15 percent of reading, whichever is greater. The cone static pressure was measured with a 5-psid fast-response transducer, referenced to a near vacuum, and calibrated to 1-psia full scale. The precision of this transducer is estimated to be ±0.002 psi or ±1.0 percent of reading, whichever is greater.

The parachute behavior in the airstream was recorded with two high-speed 16-mm motion-picture cameras and two still cameras for both shadowgraph and direct photography.

3.0 PROCEDURE

3.1 TEST CONDITIONS

The test was conducted at a nominal Mach number of 8 (variations listed below are from tunnel calibrations) and free-stream unit Reynolds numbers from 1.1 to 3.6 million. A summary of the test conditions at each dynamic pressure is given below.

M_∞	p_o, psia	T_o, °R	q_∞, psia	p_∞, psia	$Re_\infty \times 10^{-6}$, 1/ft at T_o, °R = 860	$Re_\infty \times 10^{-6}$, 1/ft at T_o, °R = 1,220
7.94	210	860*, 1,220	1.00	0.022	1.8	1.1
7.95	265	↓	1.25	0.028	2.2	1.3
7.96	320	↓	1.50	0.034	2.7	1.6
7.97	370	↓	1.75	0.039	3.1	1.9
7.98	425	↓	2.00	0.044	3.6	2.1

*Temperature below that required to prevent air liquefaction in the test section.

A test summary showing all configurations and conditions tested along with the variables for each is presented in Table 1.

3.2 TEST PROCEDURE

Parachutes made of nylon and Kevlar 29 materials would not withstand the temperatures encountered in the normal operation of Tunnel B. For this reason, the wind tunnel was often operated at a reduced stilling-chamber temperature below that required to prevent air liquefaction in the test section.

The first test phase was the captive parachute testing. The parachute was attached to the balance in the forebody cone by means of a riser line which positioned the decelerator at a specified X/D distance from the base of the cone. The test procedure used was to allow the chute to hang free from the balance when injected into the tunnel flow. Upon injection, high-speed movie cameras and a visicorder which recorded the drag input from the balance were run for a designated length of time. If the parachute had not failed after reaching the centerline of the tunnel, several seconds of continuous force data were taken. Still pictures were taken when the force data were obtained.

Wake survey data were also obtained downstream of the forebody cone by use of the VKF X-Y-Z overhead probe drive mechanism which permitted the probe to be moved independently of the forebody and supports. The wake surveys, at various X/D locations, were made in four vertical planes parallel to the forebody axis of symmetry at lateral displacements of 0.0, 1.15, 2.25, and 4.0 in.

3.3 DATA REDUCTION

Main balance force data were reduced in the body axis system. Drag was calculated by the equation

$$\text{Drag} = \left[(F_N)^2 + (F_Y)^2 + (F_A)^2 \right]^{0.5}$$

which is the resultant force along the riser lines of the parachutes measured by the balance.

A statistical method was used to analyze the decelerator drag data which were recorded at a rate of approximately 800 samples per second. The method provides a means of evaluating the drag dynamics of each decelerator tested by calculating Gaussian distribution parameters from each group of data (see Ref. 3). The calculated parameters are average drag coefficient (C_{D_o}), standard deviation (DEV), skewness, and kurtosis.

The average drag coefficient is the most probable value in the drag coefficient distribution and is determined by the equation

$$C_{D_o} = (1/N) \sum_{i=1}^{N} C_{D_i}$$

Standard deviation measures the spread of the distribution and is calculated by

$$DEV = \left[(1/N) \sum_{i=1}^{N} (C_{D_i} - C_{D_o})^2 \right]^{0.5}$$

Skewness is a measure of the asymmetry of the distribution determined by

$$\text{Skewness} = \left[1/N \ (DEV)^3 \right] \sum_{i=1}^{N} (C_{D_i} - C_{D_o})^3$$

Kurtosis is a measure of the peakedness of the data and was found by the equation

$$\text{Kurtosis} = \left[1/N \ (DEV)^4 \right] \sum_{i=1}^{N} (C_{D_i} - C_{D_o})^4$$

The value of N is the total number of drag coefficient data samples in a group of data. This value decreased from approximately 1,600 to 700 samples per group as the test progressed, and on-line evaluation of the parachute drag dynamics showed the sample size could be reduced.

To compare drag dynamics of one decelerator with those of another, it is necessary to determine a relative dynamic parameter (RDP). This value is calculated by determining a 95-percent probability interval and dividing this interval by C_{D_o}. In equation form, RDP = $(Z_1 + Z_2)$ (DEV)/C_{D_o} where Z_1 and Z_2 are parameters derived from the skewness and kurtosis values (see Ref. 3) representing a factor of the 95-percent probability interval limits (see Appendix II, Ref. 4 for additional information concerning this method).

The significance of the relative dynamics parameter (RDP) can be readily understood by explaining the drag dynamics of a decelerator when values of zero, unity, and two are assigned to the RDP. A value of zero implies no dynamics, a value of unity implies that the magnitude of dynamics about the average is equal to 50 percent of the average drag

coefficient, and a value of two implies that the magnitude of dynamics about the average drag coefficient value is equal to 100 percent of the average drag coefficient. The relative drag parameters of the various parachute configurations tested are presented in Table 1.

3.4 DATA PRECISION

An evaluation of the influence of random measurement errors is presented in this section to provide a partial measure of the uncertainty of the final test results presented in this report.

3.4.1 Test Conditions

Uncertainties in the basic tunnel parameters p_o and T_o (see Section 2.3) and the two-sigma deviation in Mach number determined from test section flow calibrations were used to estimate uncertainties in the other free-stream properties, using the Taylor series method of error propagation.

	Uncertainty (±), percent					
M_∞	M_∞	p_o	T_o	p_o'	p_∞	q_∞	Re_∞
7.94	0.4	0.1	0.4	1.7	2.4	1.7	1.2
7.95	0.4	0.1	0.4	1.7	2.4	1.7	1.2
7.96	0.3	0.1	0.4	1.2	1.6	1.1	1.0
7.97	0.3	0.1	0.4	1.2	1.6	1.1	1.0
7.98	0.3	0.1	0.4	1.2	1.6	1.1	1.0

3.4.2 Test Data

The basic precision of the wake parameter and drag coefficients was computed using the measurement precision values listed in Section 2.3 with the assumption that the free-stream flow nonuniformity is a bias type of uncertainty which is constant for all test runs.

	Precision (±) Measured Values			
M_∞	p_t/p_o	p_s/p_∞	T_T/T_o	C_D
7.94	0.017	0.122	0.006	0.008
7.95	0.017	0.110	0.006	0.007
7.96	0.012	0.081	0.006	0.005
7.97	0.012	0.076	0.006	0.005
7.98	0.012	0.072	0.006	0.004

The uncertainty in forebody angle of attack, as determined from tunnel sector calibrations and consideration of the possible errors in model deflection calculations, is estimated to be 0.1 deg. No estimate has been made to take into account strut and cone deflection attributable to heating from the tunnel flow.

Estimates of precision of measurement as given above are normally considered a measure of the repeatability to be expected in the test results. For these parachute data, however, two factors which can greatly influence the results and hence the data repeatability should be noted. These are (1) the degree of similitude achieved in the parachute models each of which is individually hand made and (2) the initial behavior (dynamics) of the model during the injection sequence which could have an unobservable effect upon the material properties and structural integrity before data taking begins.

4.0 RESULTS AND DISCUSSION

Surveys of the forebody wake were made to determine the local flow-field conditions in which the parachutes were tested. These vertical surveys consisted of pitot and static pressure and total temperature profiles, and these are presented in Figs. 5 through 7. All wake survey data were obtained at T_o = 1,220°R.

The present data obtained along the vertical plane of symmetry of the forebody (Y/D = 0) at q_∞ = 1.0 psia are compared with similar data from a previous test (Ref. 1) in Fig. 5. The data in Ref. 1 were obtained at T_o = 1,220 and 860°R using the same forebody and support system; the data for both temperatures are presented in the figure. The pitot and static pressure profiles were in good agreement with the previous data (Fig. 5a and b), and the total temperature profiles agreed well at X/D = 3.0 and 4.0 (Fig. 5c). At X/D = 2.0, the temperature profiles were in good agreement outside the wake shock (Z/D > 0.3), but differences were evident at Z/D < 0.3 for all three sets of data. These differences were attributed to the effects of Reynolds number on the temperature probe recovery characteristics (probes were not calibrated) which were not evaluated in either test; furthermore a different probe was used in the present tests.

The effects of varying dynamic pressure on the wake survey profiles are illustrated in Fig. 6 for Y/D = 0. The pressure profiles were unaffected as shown in Figs. 6a and b. Slight changes in level of the temperature profile inside the wake shock were observed (Fig. 6c). These levels increased with q_∞, which again is an indication of Reynolds number effect on the probe response.

Pressure and temperature profiles obtained at various lateral survey stations are presented in Fig. 7. The pressure profiles (Figs. 7a and b) at Y/D = 0.38 and X/D = 3.0 showed a disturbance near Z/D = 0, which indicates the wake shock location in the horizontal plane. The disturbances at Y/D = 0.67, X/D = 2.0 and 3.0, and Z/D ~ 0.5 were caused by flow disturbances from the top right strut (view looking upstream) supporting the forebody.

Selected results of the parachute tests are presented in Figs. 8 through 11 in terms of average drag coefficient (C_{D_o}) and relative dynamic parameter (RDP). A complete summary of these data is presented in Table 1.

The drag and dynamic characteristics of various Kevlar 29 parachute configurations at X/D = 5.0 are presented in Figs. 8a and b, respectively. Data are shown for two decelerator designs with two canopy diameters. Generally, the smaller parachutes developed a higher drag coefficient over the dynamic pressure and axial location ranges, and the drag coefficients did not vary as much with q_∞ as did the results for the 8-in. parachutes. All configurations approached similar drag coefficient levels at the higher dynamic pressures. Figure 8b shows the high dynamic instabilities encountered on the 8-in. parachutes near q_∞ = 1.25 psia.

The drag and dynamic characteristics of Kevlar 29 parachute configuration 250-777 at several X/D locations are illustrated in Fig. 9 for T_o = 860°R. In general, the drag coefficient (Fig. 9a) was maximum at the most aft trailing distances ($X/D \geq 4.5$), where the effects of q_∞ were also minimal. At all X/D locations, increasing q_∞ generally increased C_{D_o}. The dynamic characteristics tended to decrease with increasing X/D and q_∞ as shown in Fig. 9b.

Results at the two free-stream temperature conditions for a Kevlar 29 configuration are given in Fig. 10. The limited wake survey data available (see Fig. 5) showed little effect of temperature (increase in Re_∞ at reduced T_o) on the pressure profiles, and the differences obtained in the parachute characteristics may have been caused by temperature effects on the parachute material properties.

The effects of varying the material, and hence the stiffness and porosity, of a configuration 250 parachute at X/D = 4.0 and T_o = 860°R are shown in Fig. 11. For these conditions, the Kevlar parachute had the highest drag coefficient and slightly higher dynamics. The BBB parachute had the most uniform variation of C_{D_o} and RDP with q_∞ and produced about the same drag level as nylon at the higher q_∞ values. This figure also shows a comparison between the present drag data and corresponding data from Ref. 1 for the nylon parachutes. These data were in good agreement

in trend, and although the C_{D_0} was lower for the present data at the higher q_∞ values, the agreement was within the data repeatability observed in Ref. 1.

It should be noted that 26 parachutes were used in this test and that only five of these survived. Photographs of two typical parachute failures (280 configurations) are presented in Fig. 12. Some models were lost during the injection sequence because of initially high dynamics. The larger (8-in.-diam) parachutes were particularly vulnerable, and testing on these was restricted to the more aft trailing distances (X/D > 4.0). Typical shadowgraphs with parachutes in the forebody wake are shown in Fig. 13.

5.0 CONCLUDING REMARKS

The results of the wake survey and decelerator investigation may be summarized as follows:

1. For the most part, the wake survey pressure and temperature profiles agreed with the previous data obtained in Ref. 1 using the same forebody cone and support system.

2. Generally, decelerator drag increased with increasing axial location and/or increasing free-stream dynamic pressure.

3. Typically, parachute design 2 developed slightly more drag than design 5, over the X/D and q_∞ ranges.

REFERENCES

1. Lutz, R. G. and Rhudy, R. W. "Drag and Performance of Several Aerodynamic Decelerators at Mach Number 8." AEDC-TR-70-143 (AD873000), August 1970.

2. Test Facilities Handbook (Tenth Edition). "von Karman Gas Dynamics Facility, Vol. 4." Arnold Engineering Development Center, May 1974.

3. Hahn, Gerald J. and Shapiro, Samuel S. Statistical Models in Engineeering. John Wiley and Sons, Inc., New York, 1967.

4. Galigher, L. L. "Aerodynamic Characteristics of Ballutes and Disk-Gap-Band Parachutes at Mach Numbers from 1.8 to 3.7." AEDC-TR-69-245 (AD861437), November 1969.

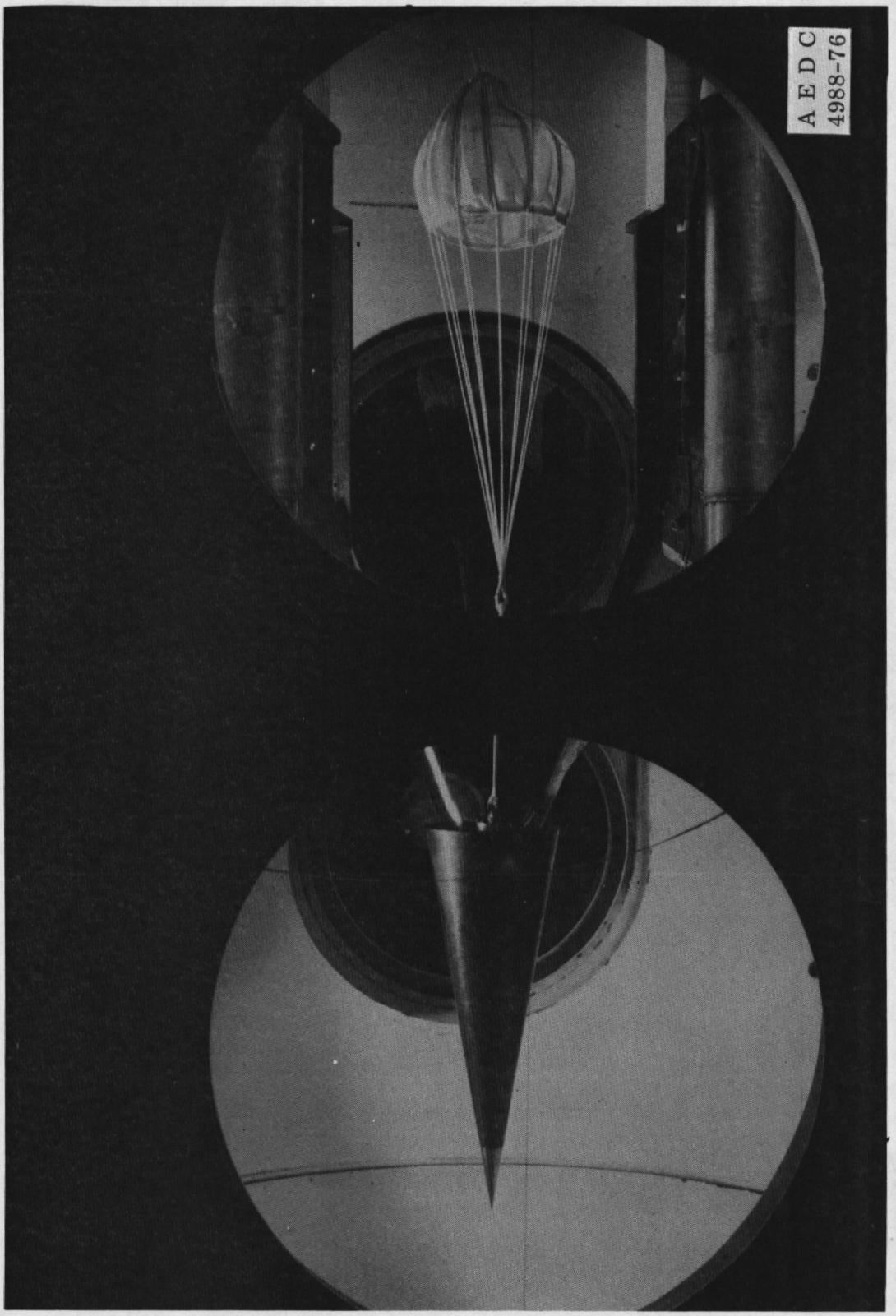

Figure 1. Configuration 580-111 installed in Tunnel B.

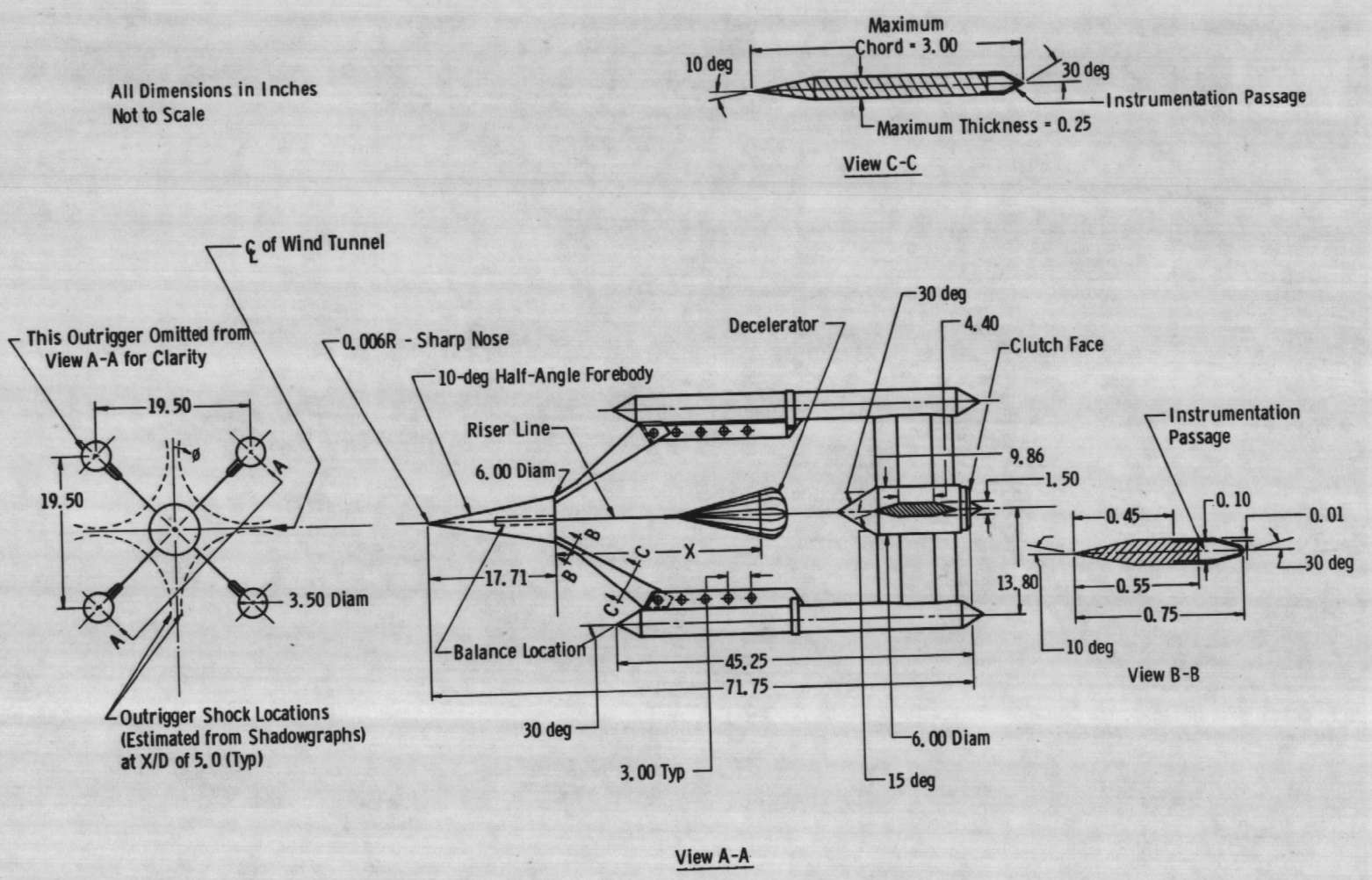

Figure 2. Forebody cone, support equipment, and decelerator location.

All Dimensions in Inches
Not to Scale

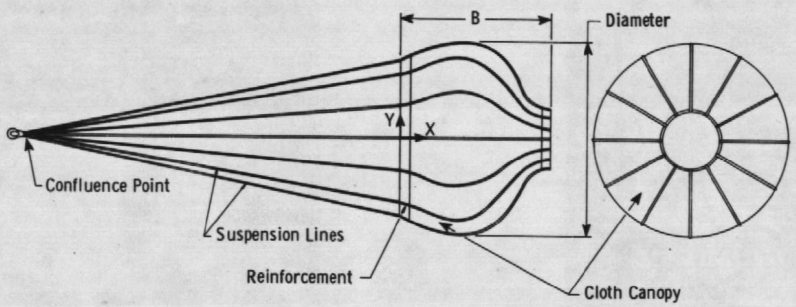

Canopy Profile Coordinates

Configuration 250		Configuration 550		Configuration 280		Configuration 580	
X	Y	X	Y	X	Y	X	Y
0	2.00	0	2.00	0	3.20	0	3.20
0.25	2.10	0.25	2.10	1.00	3.60	0.40	3.37
0.50	2.20	0.50	2.20	2.00	3.90	0.80	3.53
0.75	2.29	0.75	2.30	2.70	4.00	1.20	3.66
1.00	2.37	1.00	2.37	3.00	3.95	1.60	3.79
1.25	2.44	1.25	2.44	4.00	3.49	2.00	3.90
1.50	2.48	1.50	2.48	5.00	2.08	2.40	3.97
1.68	2.50	1.68	2.50	6.00	1.22	2.70	4.00
1.75	2.50	1.75	2.50	B=6.20	1.20	2.80	3.99
2.00	2.44	2.00	2.44			3.20	3.90
2.25	2.34	2.25	2.34			3.60	3.74
2.50	2.18	2.50	2.18			4.00	3.49
2.75	1.94	2.75	1.94			4.40	3.10
3.00	1.54	3.00	1.54			4.80	2.46
3.25	1.07	3.25	1.07			5.20	1.71
3.50	0.84	3.50	0.81			5.40	1.49
3.75	0.76	3.75	0.64			5.60	1.30
B=3.88	0.75	4.00	0.53			5.80	1.13
		4.25	0.49			6.00	1.02
		B=4.31	0.49			6.20	0.92
						6.40	0.85
						6.60	0.82
						6.80	0.79
						B=6.90	0.79

Decelerator Configuration and Material Code

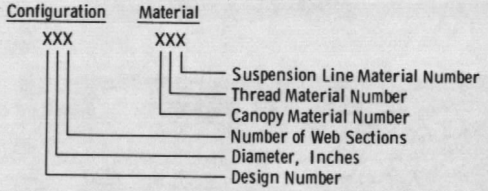

Number	Material Description
1	Nylon
4	Bisbenzimidazobenzophenanthroline
7	Kevlar 29

a. Parachute profiles and codes
Figure 3. Decelerator details.

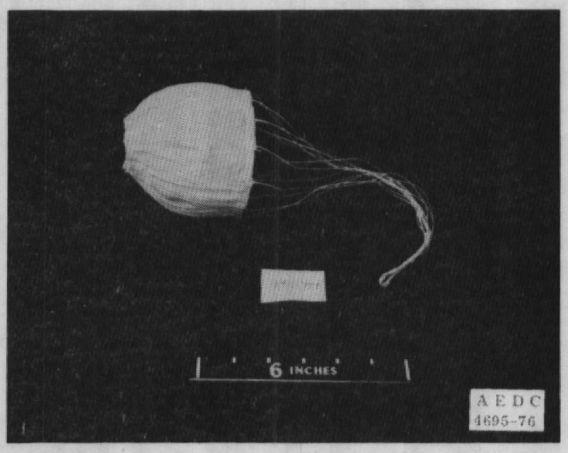

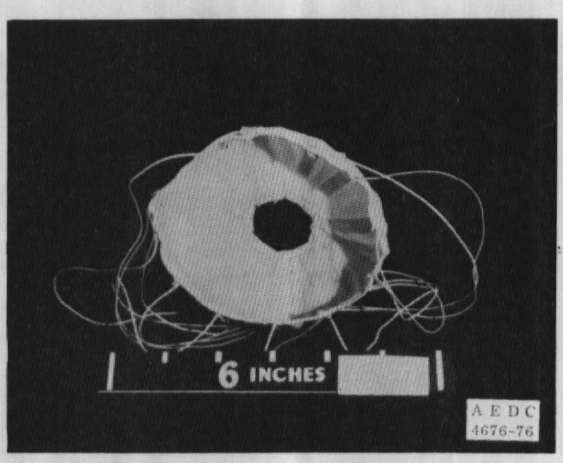

Configuration 250

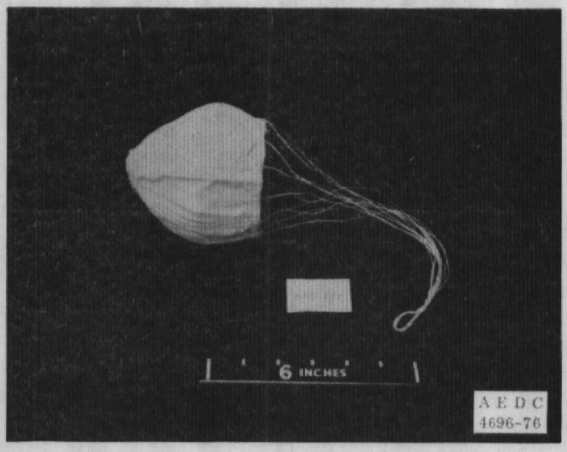

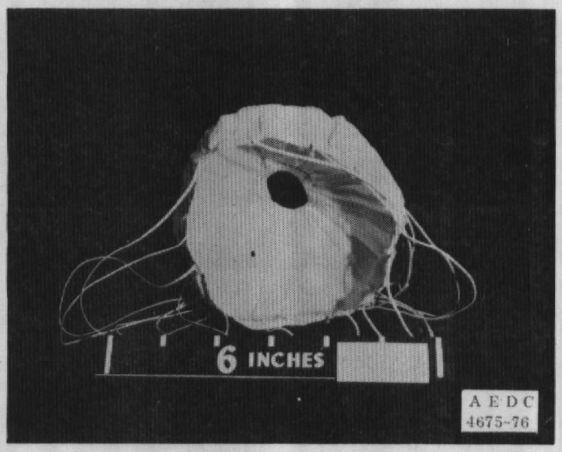

Configuration 550

b. Parachute configurations 250 and 550
Figure 3. Continued.

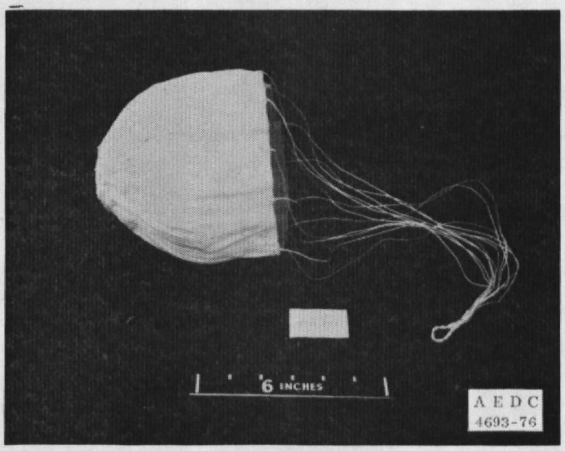

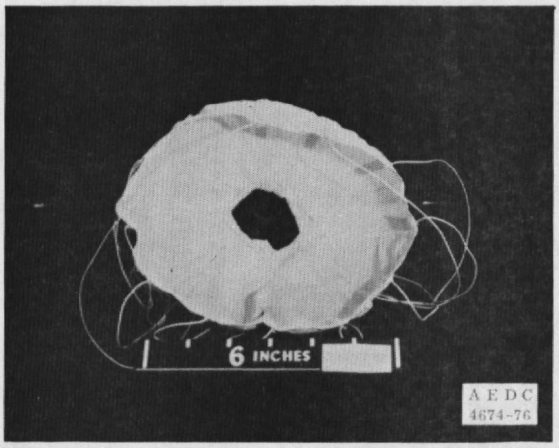

Configuration 280

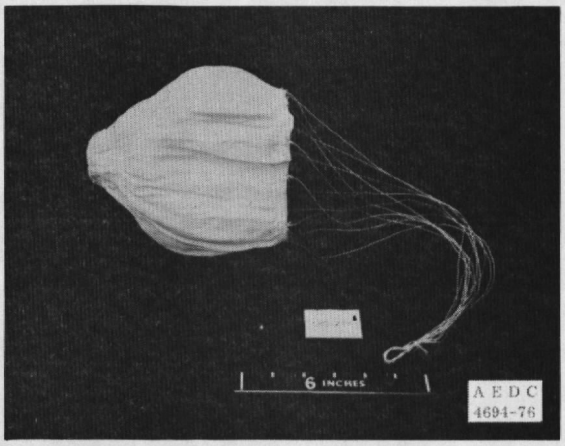

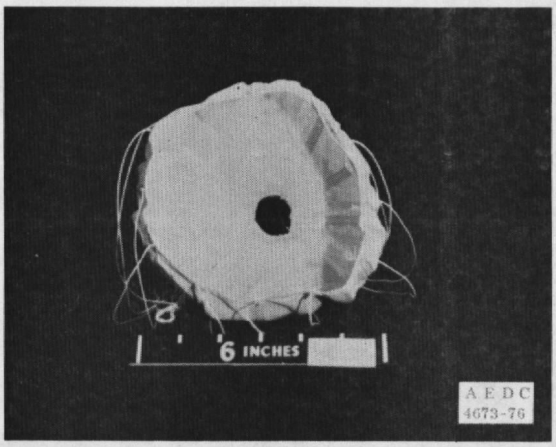

Configuration 580

c. Parachute configurations 280 and 580
Figure 3. Concluded.

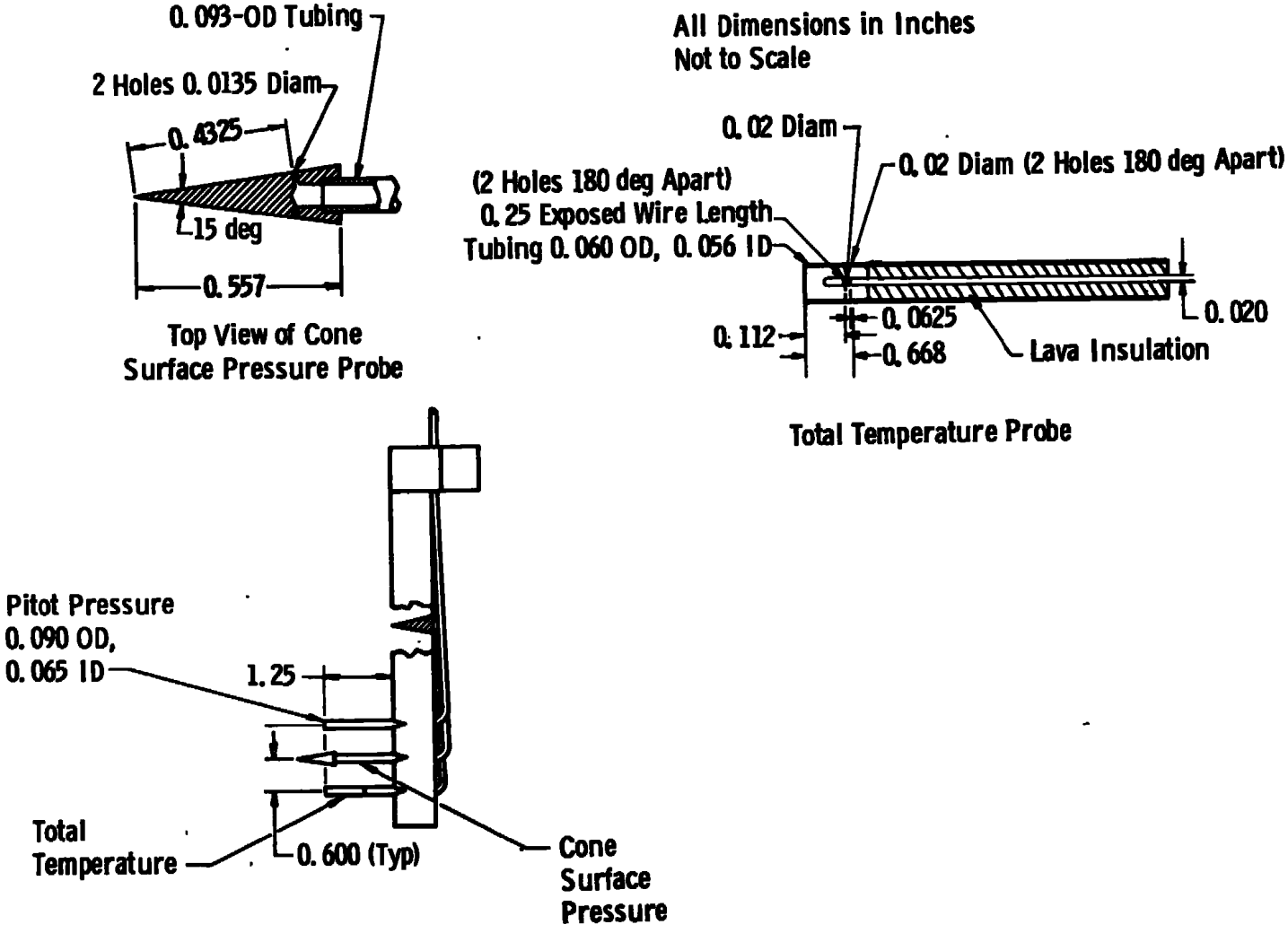

Figure 4. Wake survey rake details.

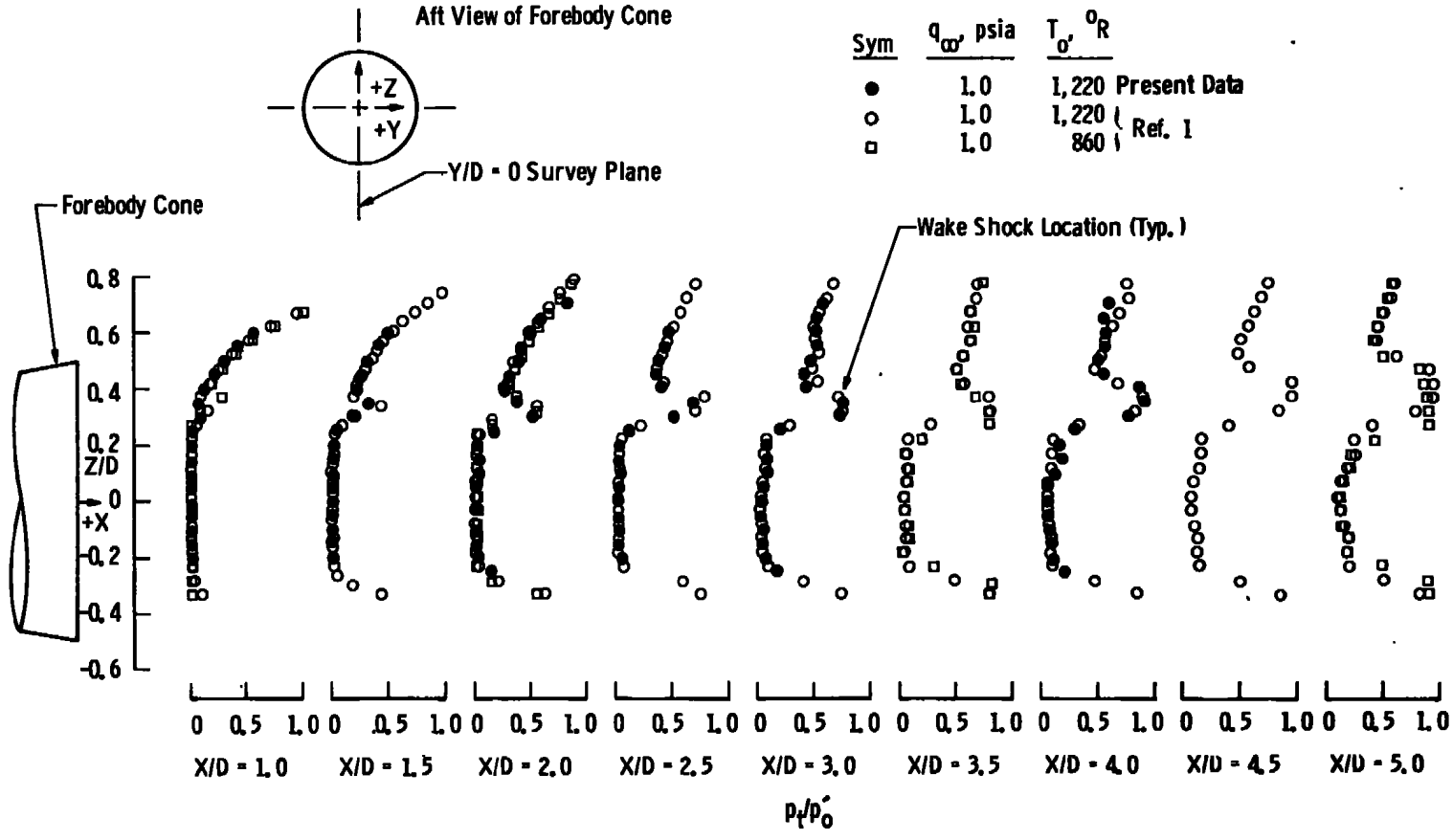

a. Pitot pressure data

Figure 5. Results of vertical surveys in the wake of the forebody cone at Y/D = 0 and q_∞ = 1.0 psia.

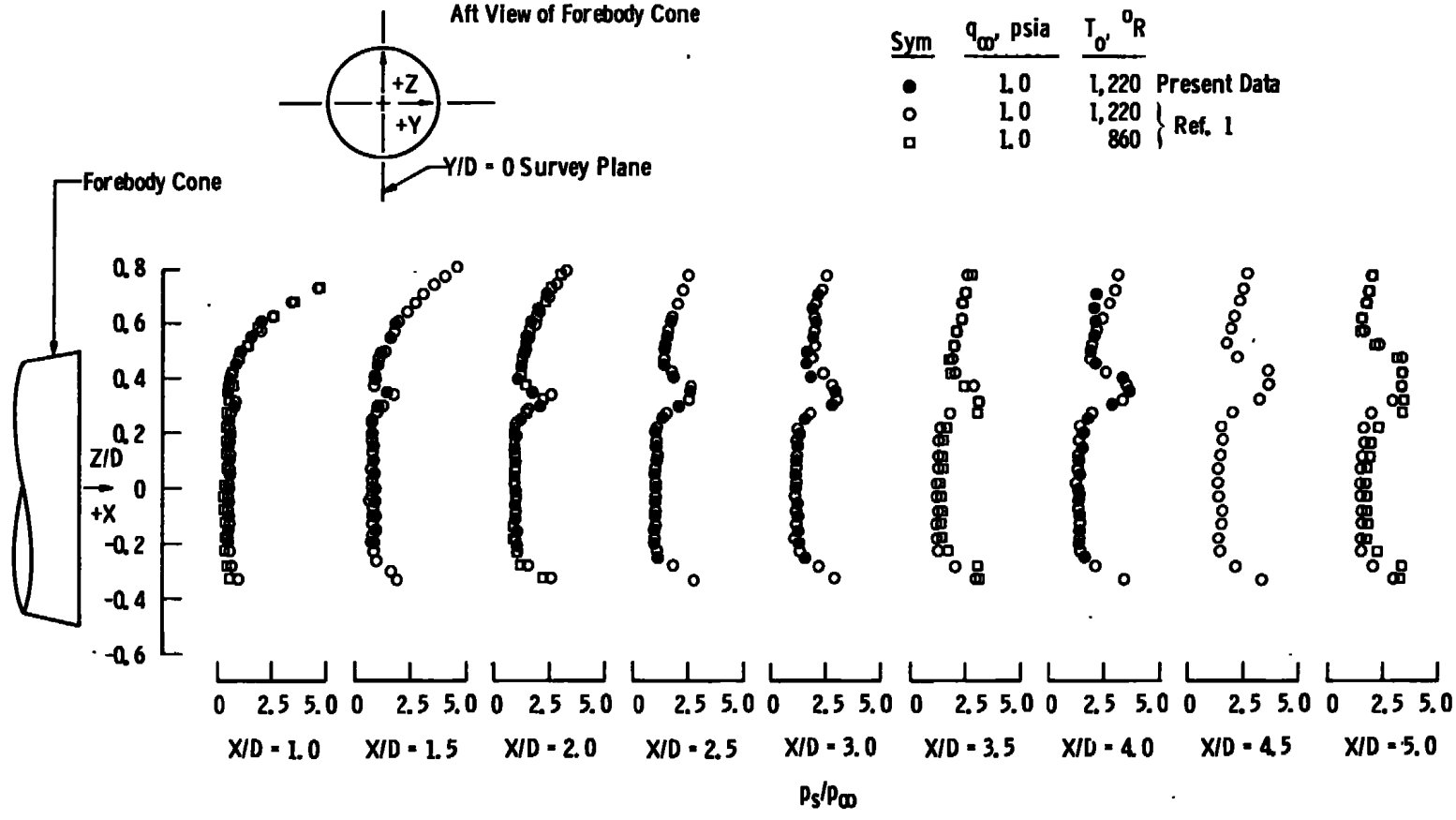

b. Static pressure data
Figure 5. Continued.

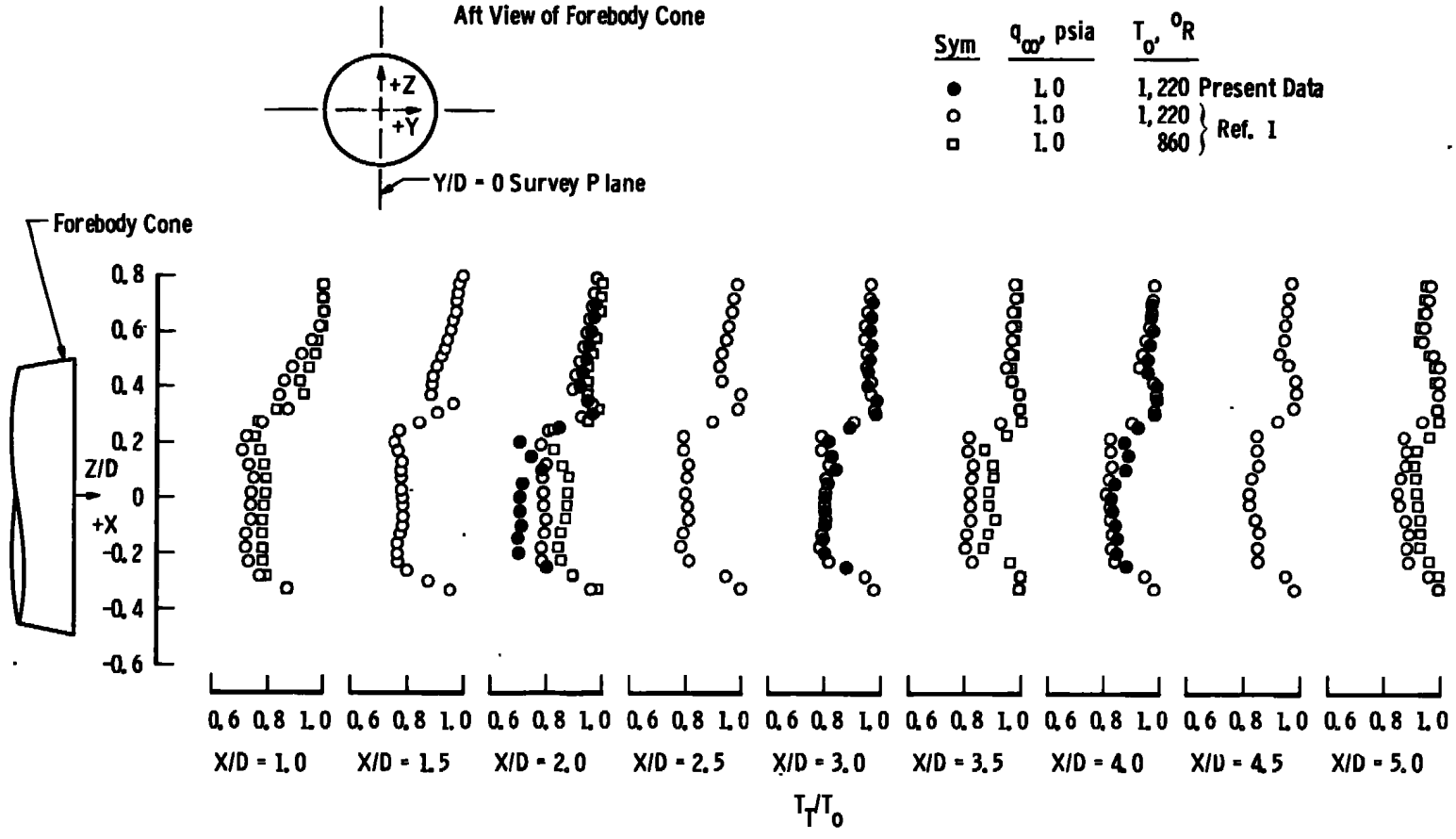

c. Total temperature data

Figure 5. Concluded.

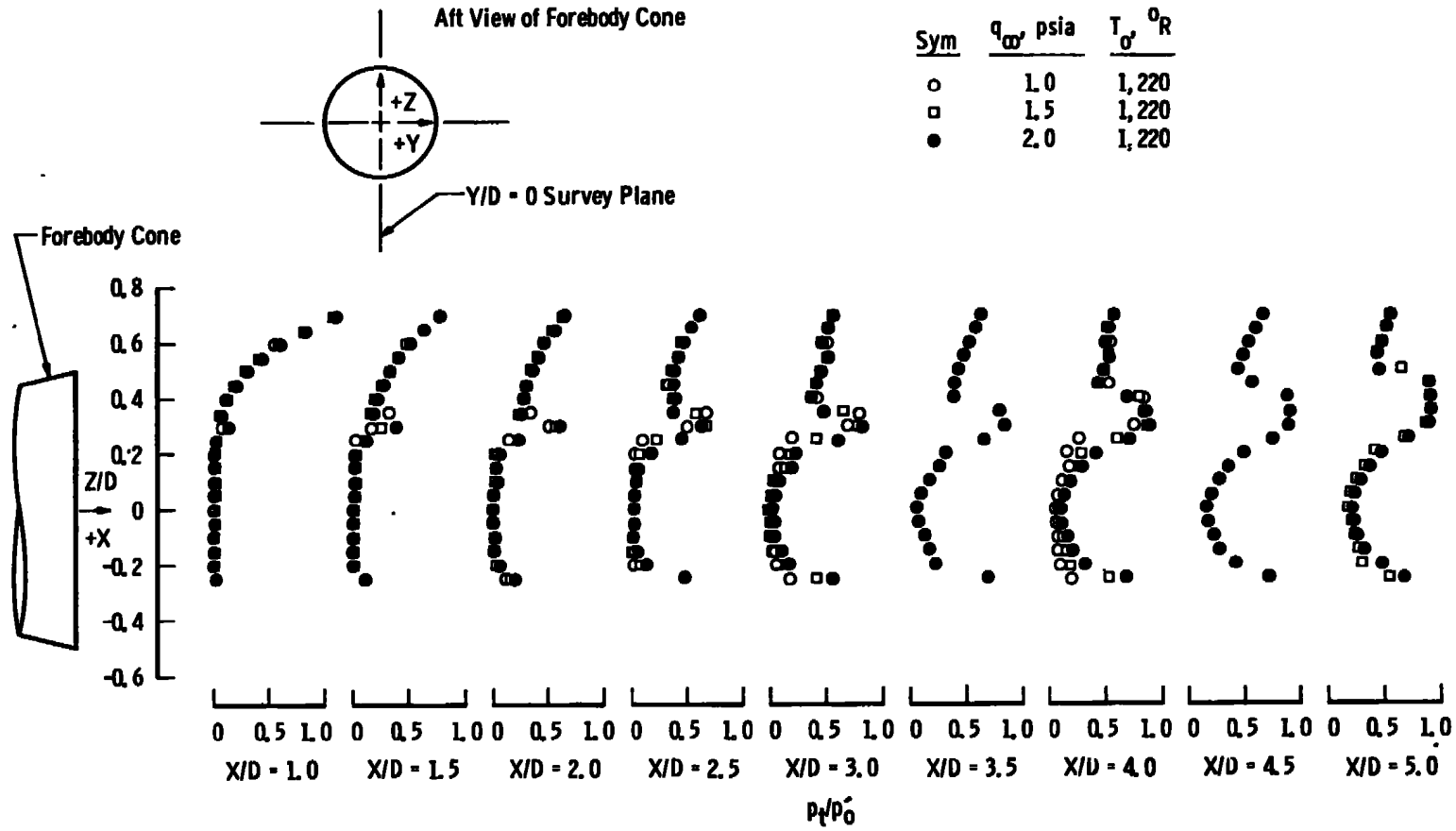

a. Pitot pressure data

Figure 6. Results of vertical surveys in the wake of the forebody cone at Y/D = 0 and various dynamic pressures.

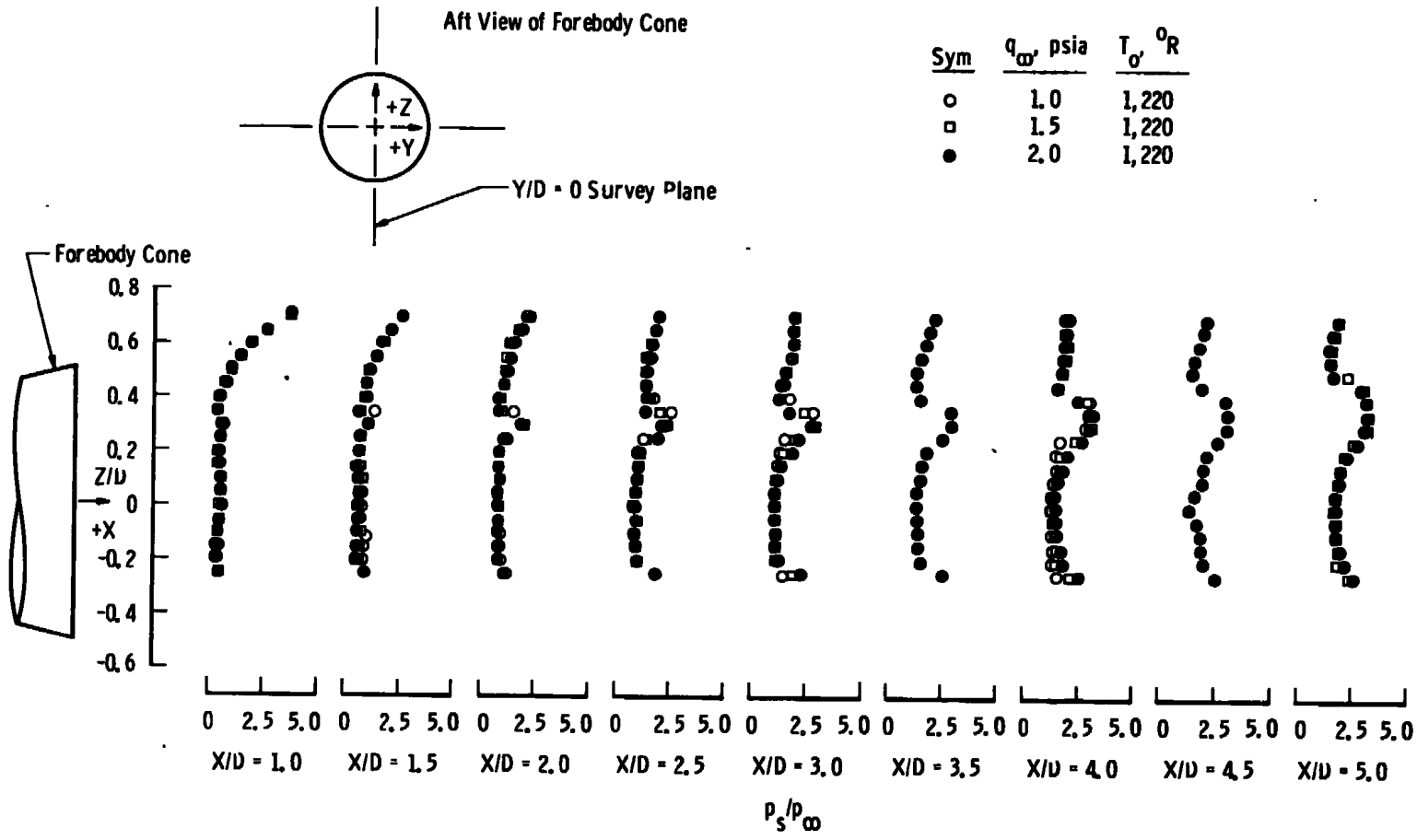

b. Static pressure data
Figure 6. Continued.

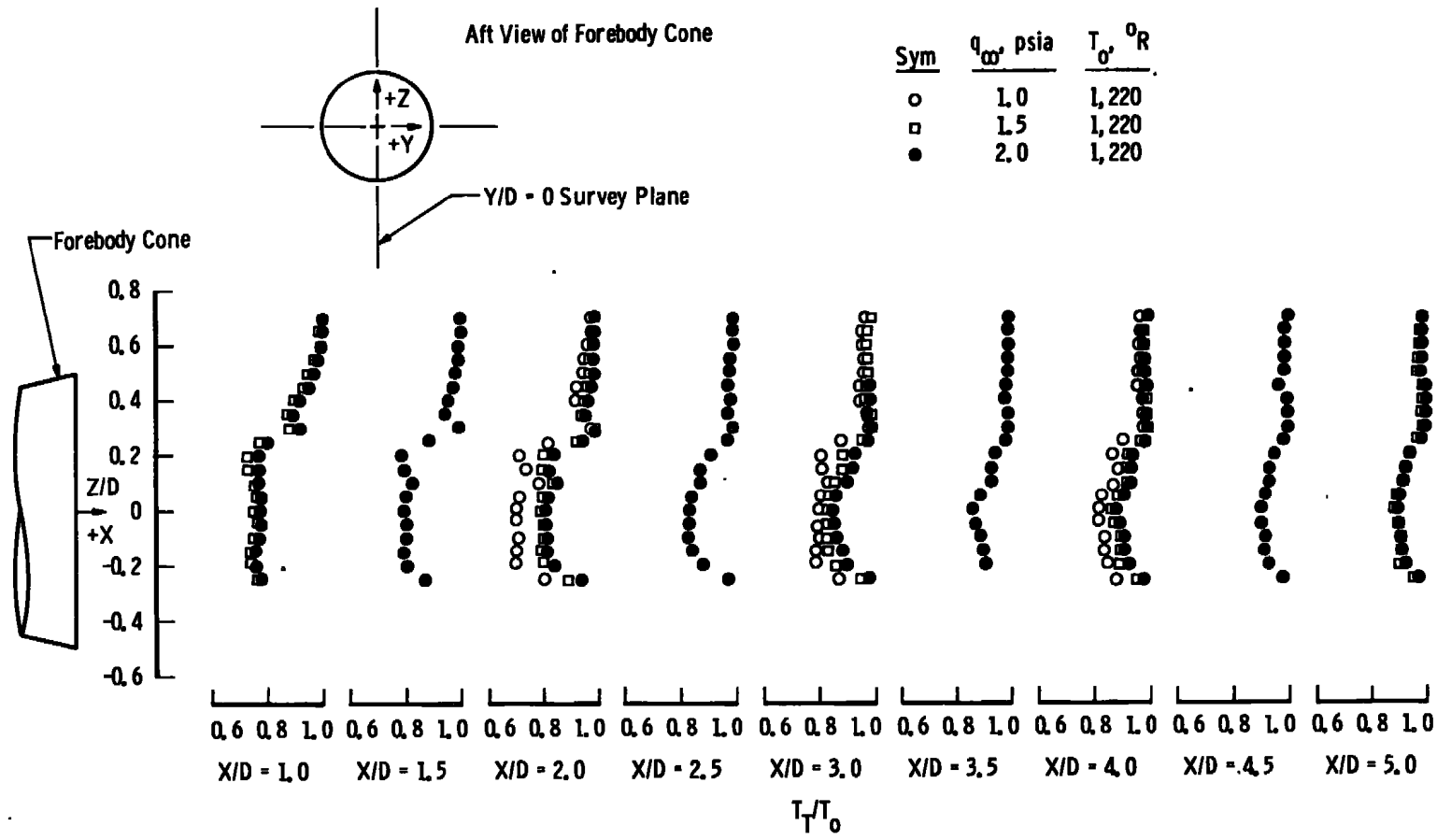

c. Total temperature data
Figure 6. Concluded.

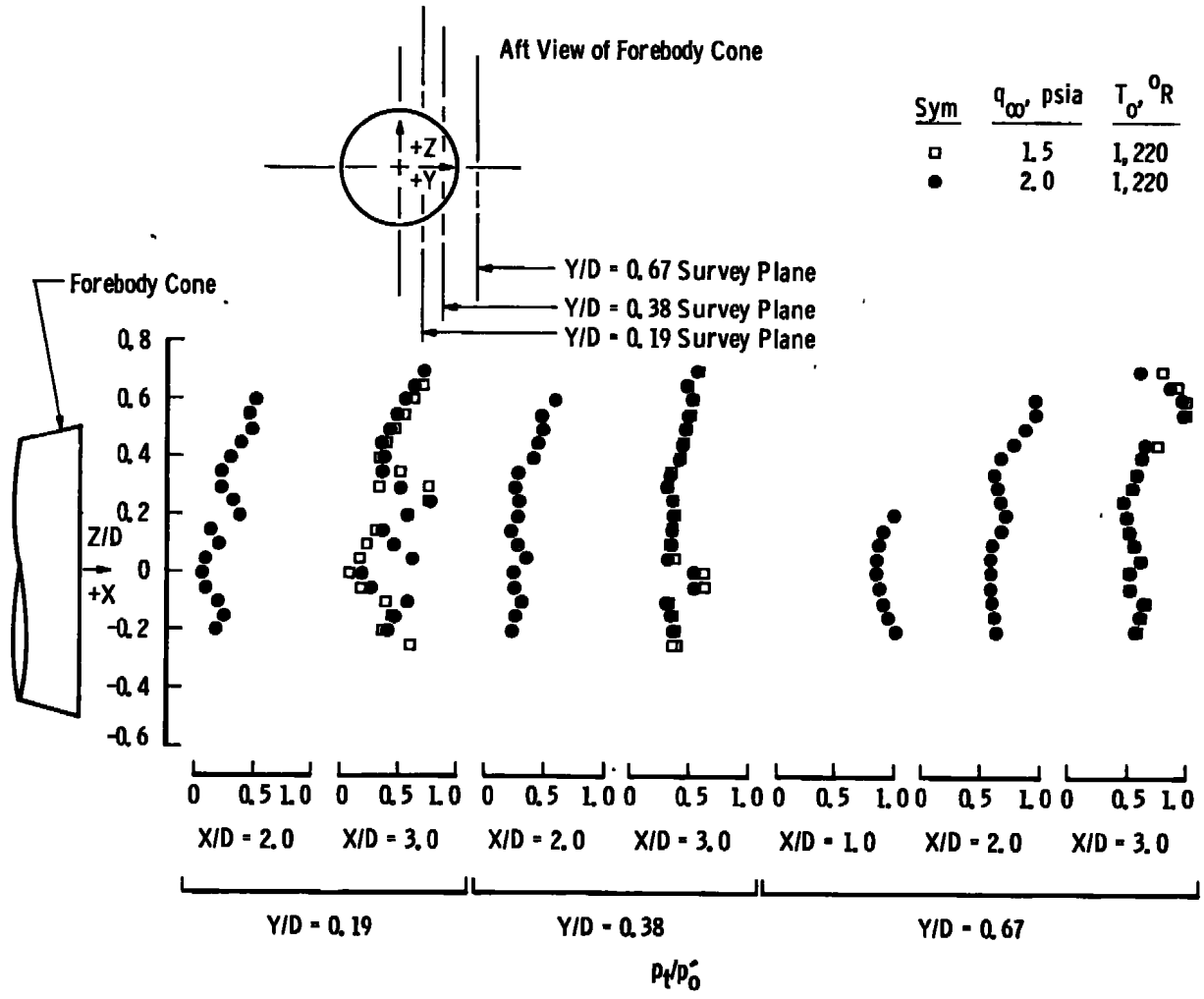

a. Pitot pressure data

Figure 7. Results of vertical surveys in the wake of the forebody cone at various Y/D locations and dynamic pressures.

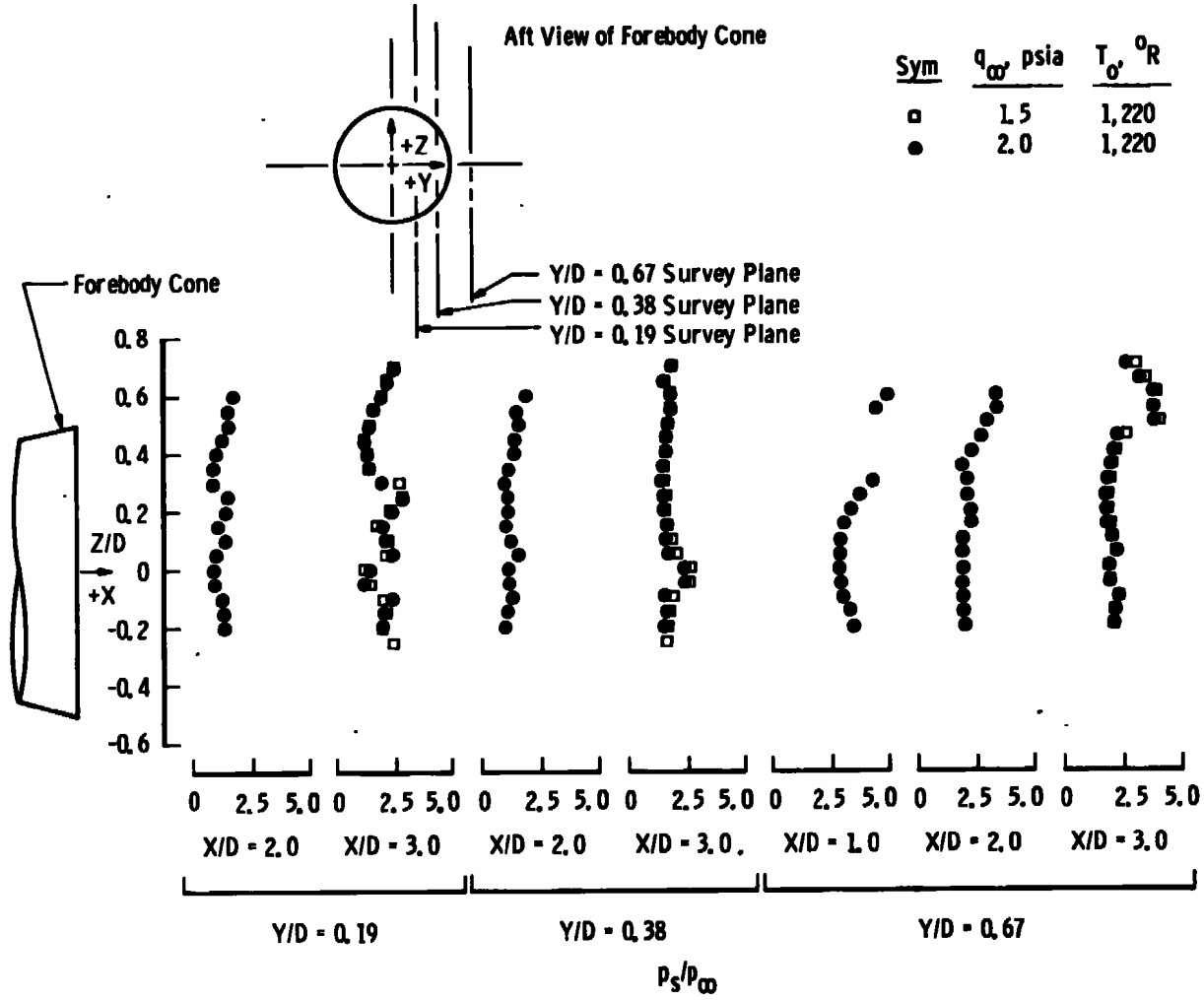

b. Static pressure data
Figure 7. Continued.

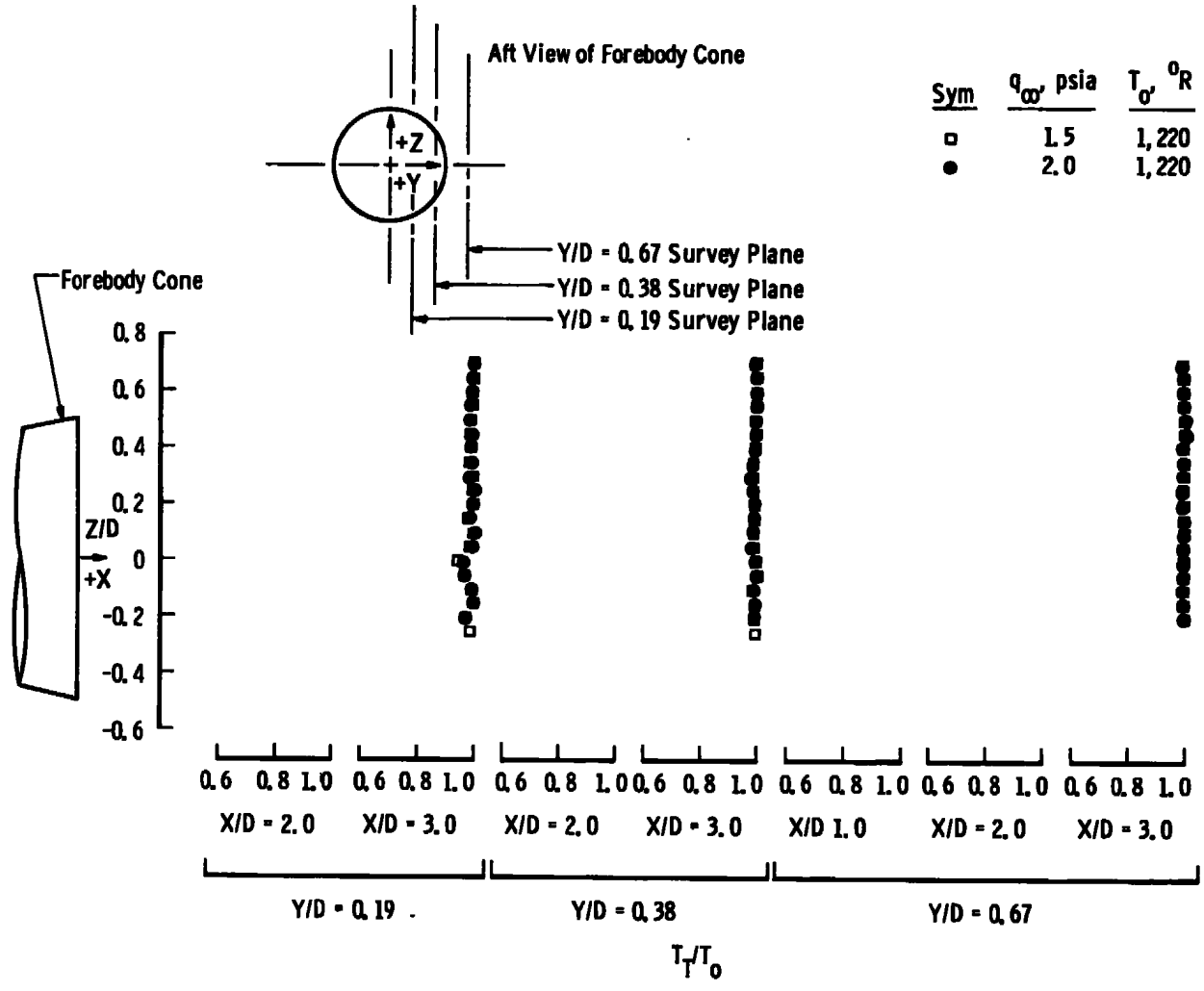

c. Total temperature data
Figure 7. Concluded.

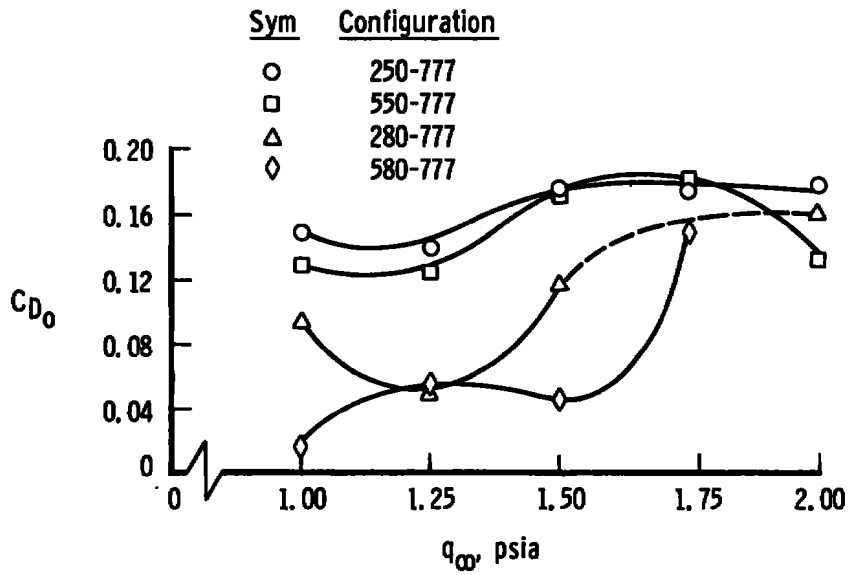

a. Drag coefficient

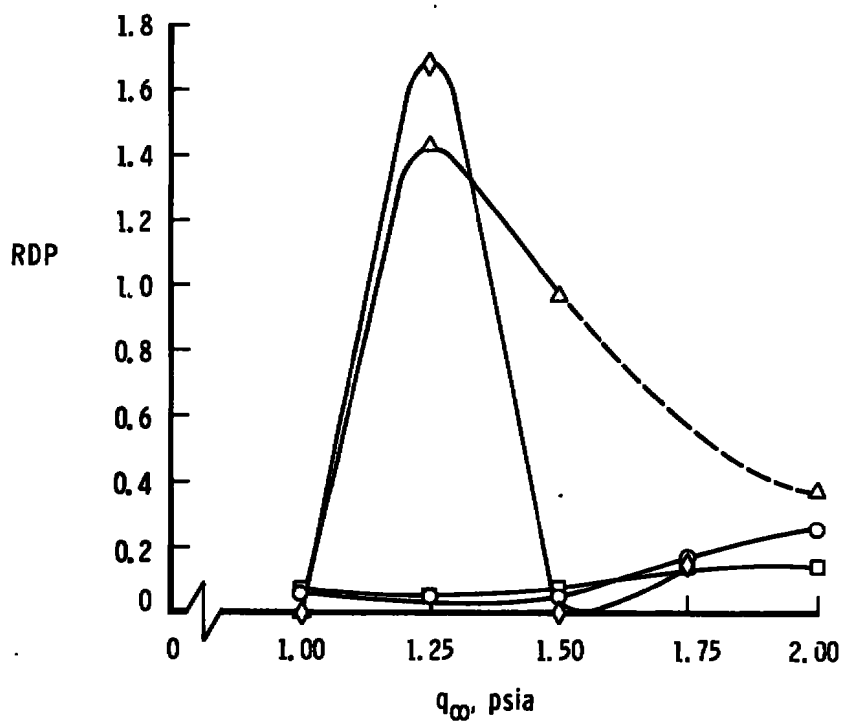

b. Relative dynamic parameter

Figure 8. Drag and dynamic characteristics of various Kevlar 29 configurations at X/D = 5.0 and T_o = 860°R.

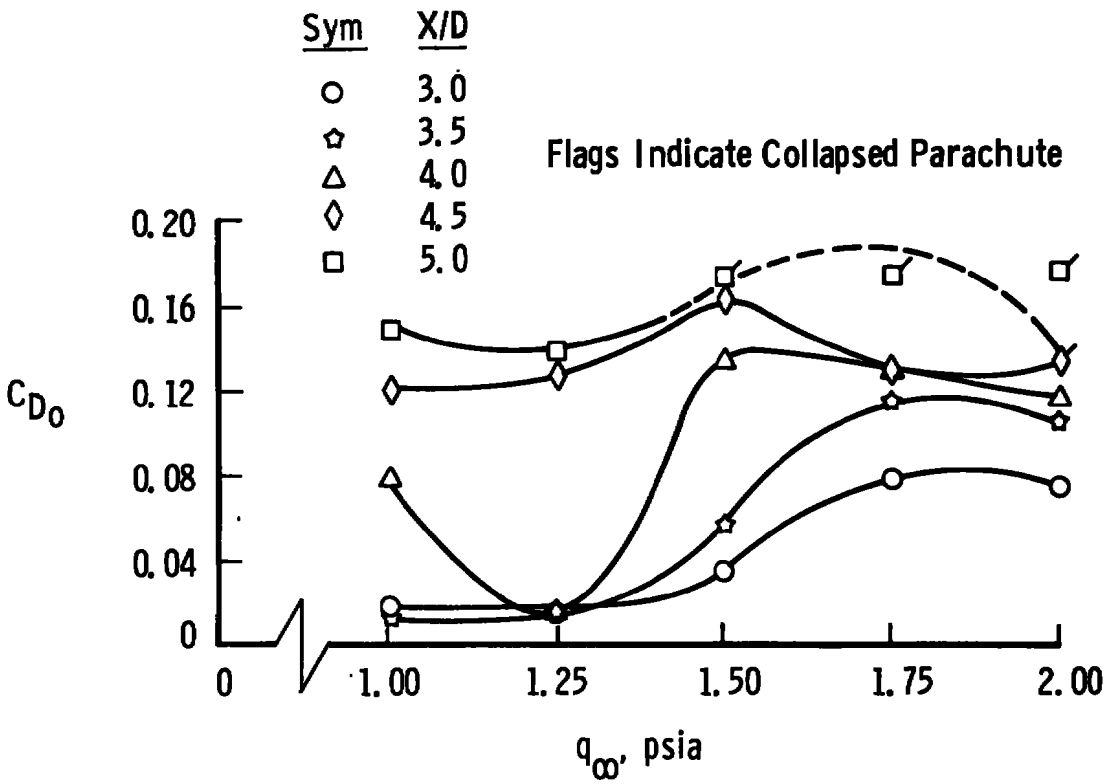

a. Drag coefficient

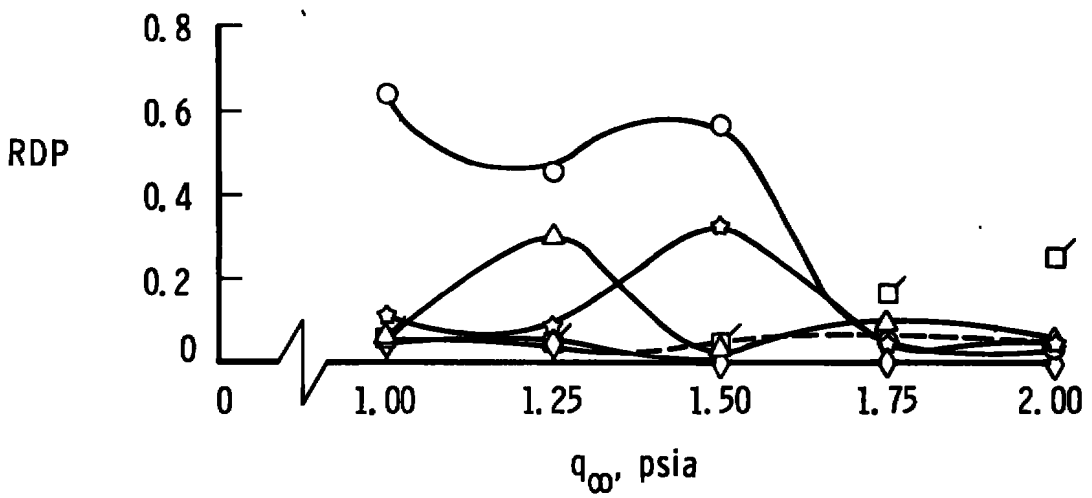

b. Relative dynamic parameter

Figure 9. Effect of X/D on Kevlar 29 parachute configuration 250-777 at T_o = 860°R.

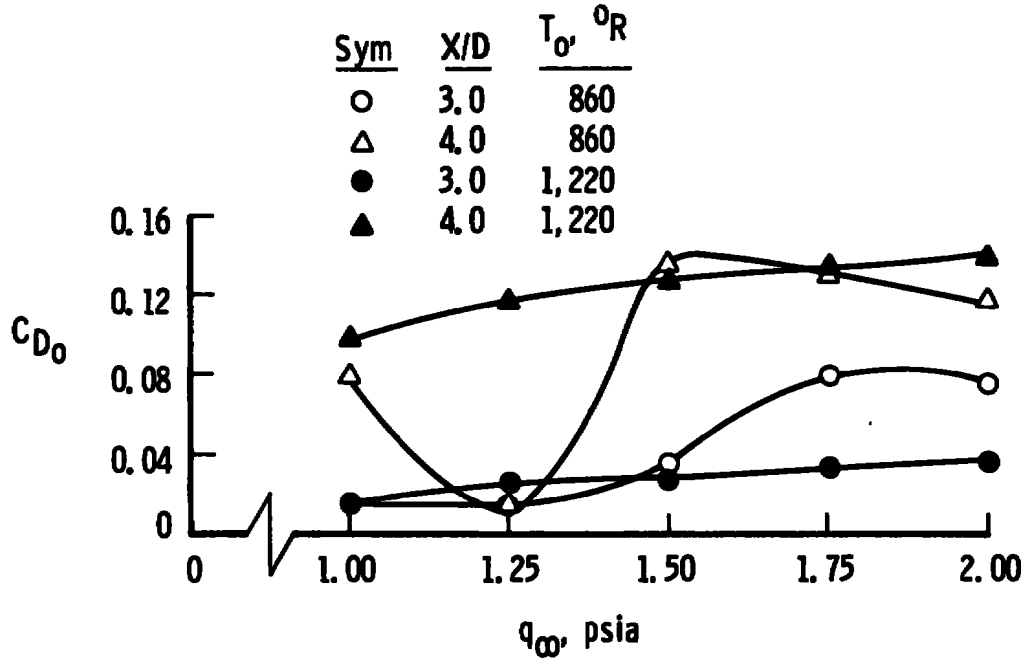

a. Drag coefficient

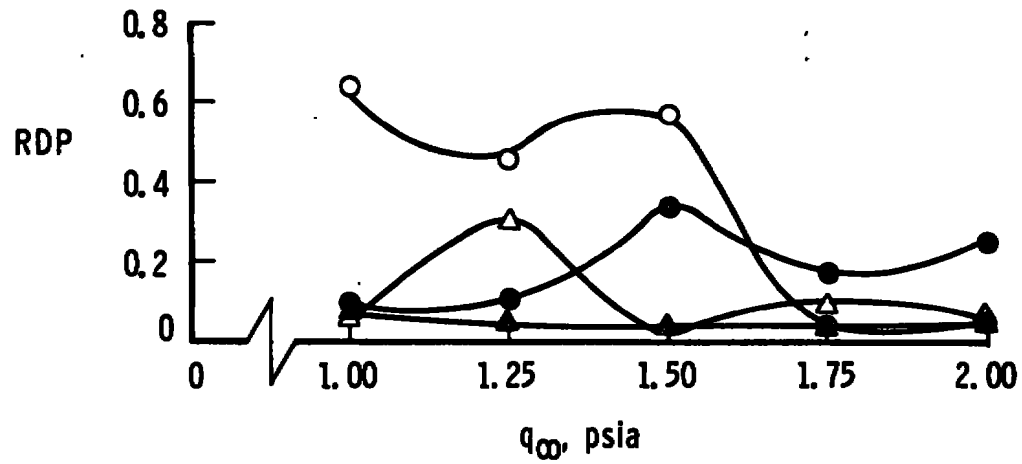

b. Relative dynamic parameter

Figure 10. Effect of T_o on Kevlar 29 parachute configuration 250-777 at various X/D's.

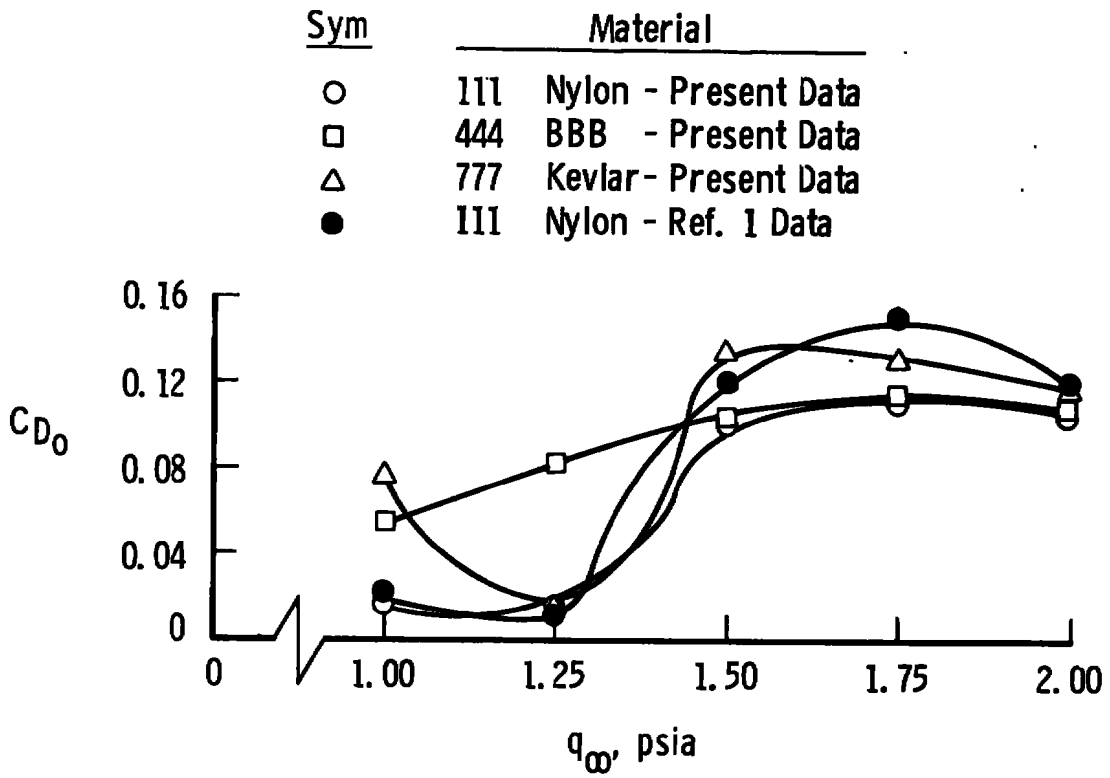

a. Drag coefficient

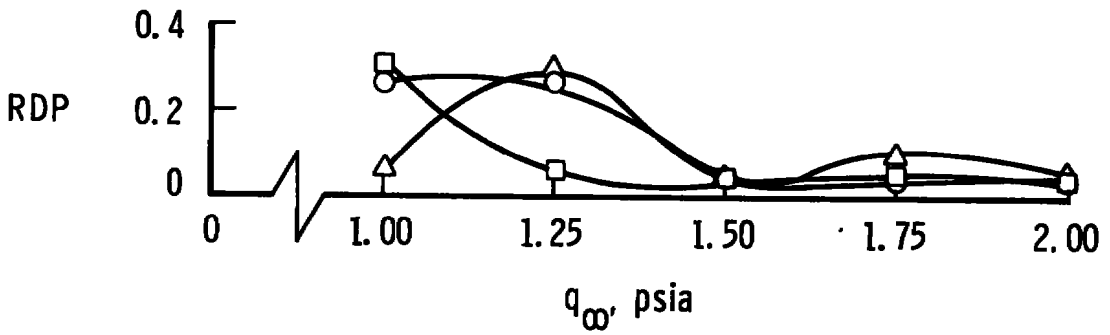

b. Relative dynamic parameter

Figure 11. Parachute material effect on configuration 250 at X/D = 4.0 and T_o = 860°R.

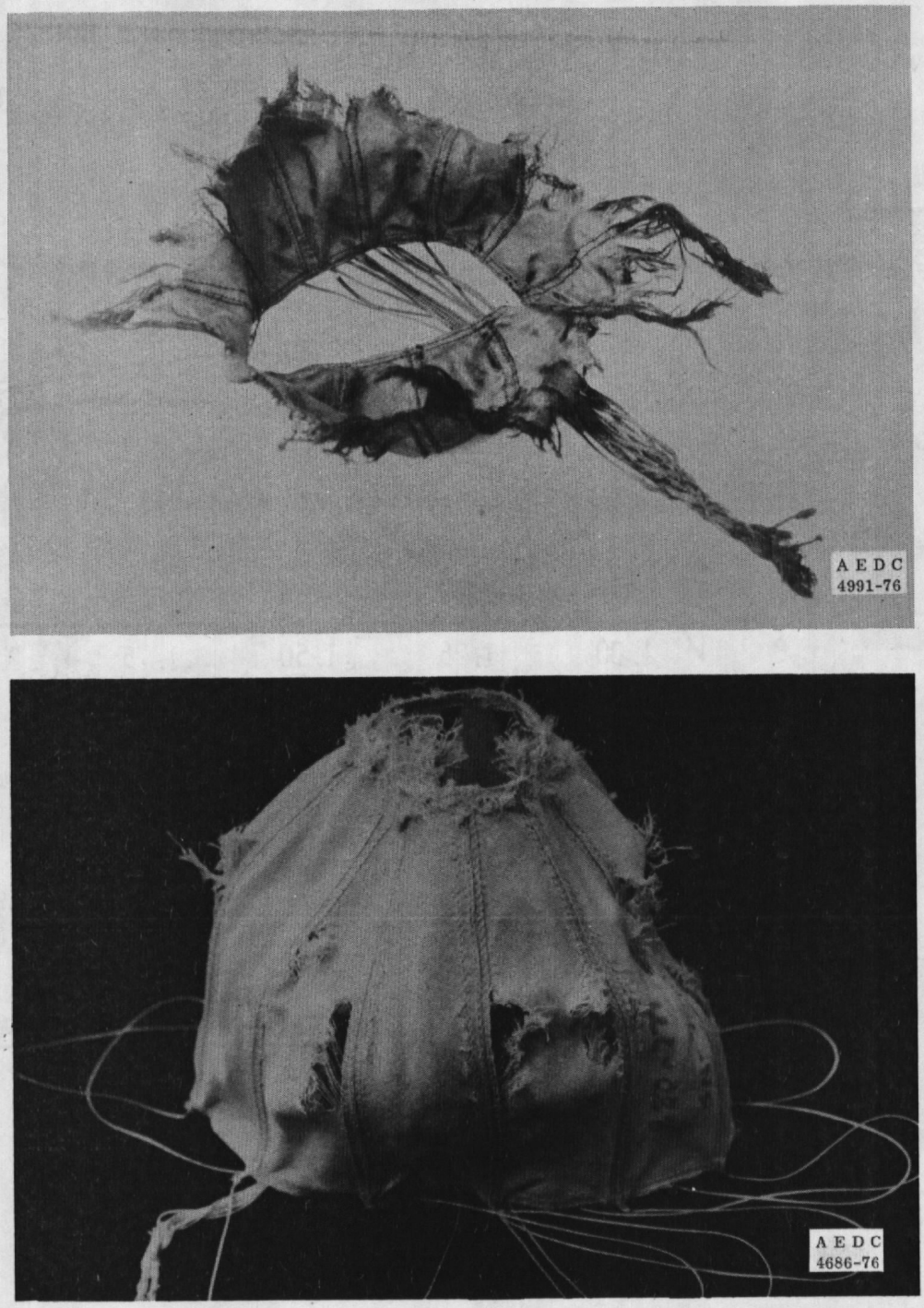

Figure 12. Typical material failures.

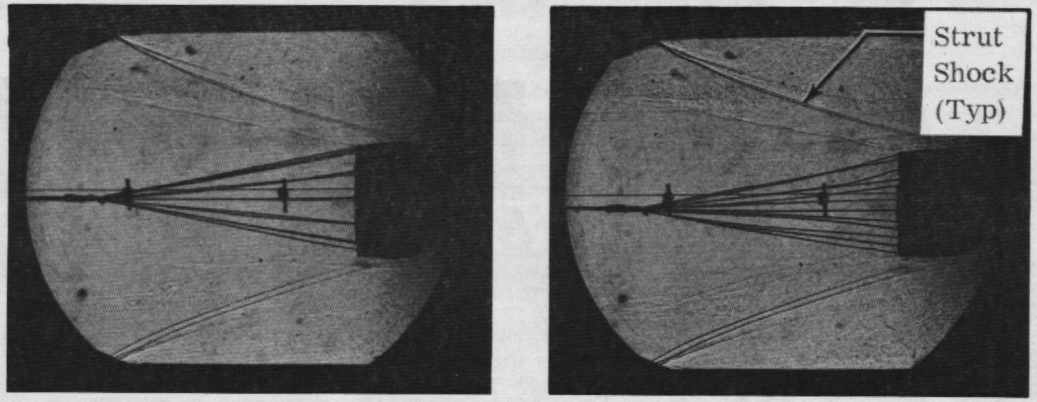

q_∞ = 1.0 psia
C_{D_o} = 0.012

q_∞ = 1.25 psia
C_{D_o} = 0.014

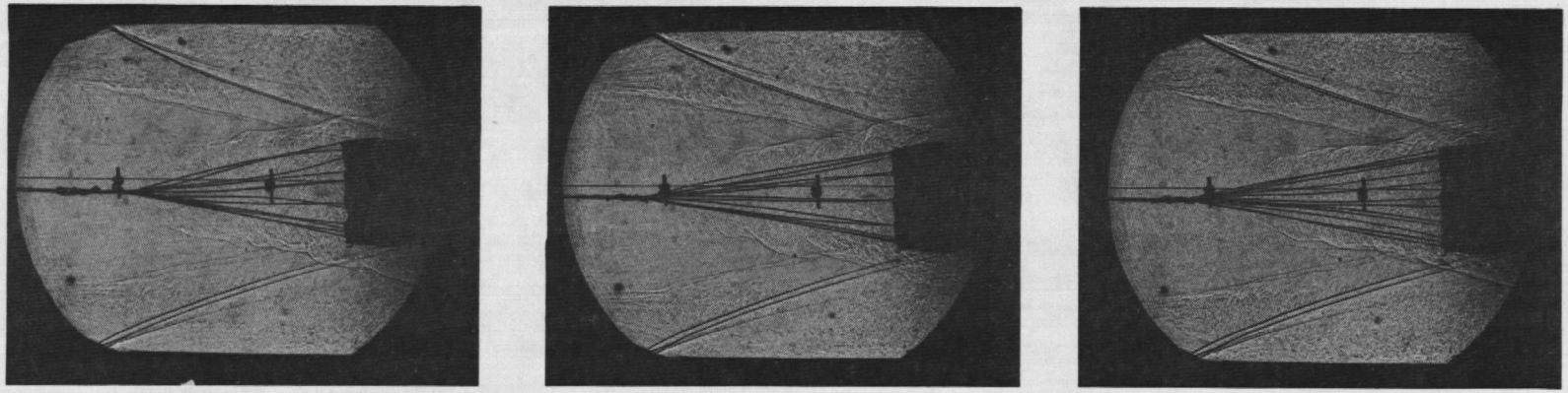

q_∞ = 1.50 psia
C_{D_o} = 0.058

q_∞ = 1.75 psia
C_{D_o} = 0.116

q_∞ = 2.0 psia
C_{D_o} = 0.106

Figure 13. Shadowgraphs of configuration 250-777 at X/D = 3.5 and T_o = 860°R.

Table 1. Test Summary — Parachute Data

Configuration			q_∞, psia																			
			1.00				1.25				1.50				1.75				2.00			
			T_o = 860°R		T_o = 1,220°R		T_o = 860°R		T_o = 1,220°R		T_o = 860°R		T_o = 1,220°R		T_o = 860°R		T_o = 1,220°R		T_o = 860°R		T_o = 1,220°R	
Design	Material	X/D	C_{D_o}	RDP	C_{D_o}	RDP	C_{D_o}	RDP	C_{D_o}	RDP	C_{D_o}	RDP	C_{D_o}	RDP	C_{D_o}	RDP	C_{D_o}	RDP	C_{D_o}	RDP	C_{D_o}	RDP
250	111	4.0	0.01719	0.2672			0.1342	0.2679			0.1008	0.04114			0.1096	0.03576			0.103	0.03485		
		5.0	0.1142	0.06635			0.1179	0.06185			0.1391	0.08719			0.09907	0			0.07238	0.09701		
	444	3.0	0.01055	0.1808	0.02025	0.1595	0.0066	0.2439	0.01965	0.1601	0.02935	0	0.03502	0.09663	0.07153	0.04795	0.03702	0.3712	0.06557	0.04452	0.042	0.6431
		3.5			0.06158	0.05508			0.07069	0.1408			0.05893	0.4008			0.07361	0.2945			0.09459	0
		4.0	0.0548	0.3118	0.1180	0.05034	0.08211	0.05934	0.1353	0.0428	0.105	0.03712	0.1287	0.04759	0.1145	0.04604	0.1372	0.04303	0.107	0.03841	0.1397	0.03386
		4.5			0.1268	0.04285			0.1634	0.03189			0.1866	0.05085			0.027	0			0.166	0.7304
		5.0	0.1188	0.0619	0.1224	0.07137	0.1139	0.06478	0.1424	0.1093	0.1691	0.1044	0.1798	0.06706	0.1538	0.1643	0.2052	0.07791	0.1373	0.1578	0.2328	0.1387
	777	3.0	0.01728	0.641	0.01618	0.09168	0.0186	0.4582	0.02687	0.1044	0.03252	0.5634	0.02743	0.3320	0.07893	0.05324	0.03462	0.1701	0.07359	0.04096	0.03618	0.2549
		3.5	0.01203	0.1129	0.06342	0	0.01442	0.08582	0.06604	0	0.05754	0.3272	0.08799	0.06047	0.1165	0.04419	0.1018	0.03832	0.1057	0.04499	0.1194	0
		4.0	0.07845	0.06352	0.1003	0.06581	0.01521	0.3012	0.1166	0.04375	0.1339	0.03959	0.1283	0.03968	0.1302	0.0953	0.1352	0.03976	0.117	0.05408	0.1395	0.0454
		4.5	0.1208	0.05935			0.1291	0.04904			0.1637	0			0.1315	0			0.1352	0		
		5.0	0.1495	0.05762	0.1369	0.05863	0.1387	0.04496	0.1597	0.08808	0.1754	0.04814	0.1797	0.05903	0.1727	0.1682	0.2088	0.04955	0.1774	0.252	0.247	0.06528
550	111	3.0	0.01107	0.1394			0.01174	0.08745			0.0204	0.8733			0.03066	0.03481			0.03133	0.03458		
		4.0	0.01261	0.1951			0.01373	0.1798			0.09823	0.02181			0.09933	0.02145			0.09224	0.02475		
		5.0	0.1085	0.06043			0.1033	0.1170			0.117	0.05464			0.1014	0.04925			0.0813	0.05566		
	444	3.0			0.01521	0.09544			0.02669	0			0.02994	0.184			0.029	0.324			0.02109	0
		3.5			0.06156	0.05471			0.07035	0.1027			0.04746	0.05122			0.06335	0.9334			0.07267	0
		4.0			0.1074	0.06186			0.1269	0.04953			0.1389	0.04055			0.1576	0.04062			0.1623	0.06638
		4.5			0.1293	0.05811															0.2729	0.06742
		5.0			0.143	0.05568			0.1404	0.06606			0.1543	0.06721			0.1655	0.06804			0.2395	0.0997
	777	3.0	0.008124	0.1181			0.1451	0.2638			0.0263	0.257			0.06181	0			0.05621	0.1916		
		3.5	0.01896	0.08575			0.01689	0			0.09288	0.03587			0.1116	0.05065			0.1081	0.05785		
		4.0	0.06323	0			0.01234	0.37			0.1446	0.04624			0.1303	0.06075			0.1261	0.06115		
		4.5	0.1133	0.06518			0.1152	0.04753			0.1625	0.03989			0.1235	0.09289			0.1186	0.1057		
		5.0	0.1291	0.07175			0.1244	0.05145			0.1719	0.07187			0.1816	0.1349			0.1316	0.1368	0.2123	0
280	111	4.5																	0.1233	0.1401		
		5.0	0.06922	0			0.0206	0			0.1214	0.05971			0.1038	0.08844			0.9616	0.06819	0.1327	0
	444	5.0			0.09589	1.288																
	777	4.0	0.02996	0			0.03333	0			0.04152	0.8492			0.09224	0.5887			0.05333	0		
		5.0	0.09249	0	0.09407	1.008	0.05061	1.444			0.1169	0.9662							0.1603	0.3639		
580	777	5.0	0.01772	0			0.05465	1.693			0.04376	0			0.1481	0.146						

NOMENCLATURE

C_D	Drag coefficient; drag force/q_∞(S)
C_{D_i}	Each individual C_D in a group of data
C_{D_o}	Average drag coefficient
D	Forebody cone base diameter (6 in.)
F_A	Total axial force, lb
F_N	Normal force, lb
F_Y	Side force, lb
M_∞	Free-stream Mach number
N	Total number of drag coefficient data samples in a group
p_o	Free-stream stagnation pressure, psia
p_o'	Calculated total pressure behind a normal shock, psia
p_s	Measured cone static pressure, psia
p_t	Measured pitot pressure, psia
p_∞	Free-stream static pressure, psia
q_∞	Free-stream dynamic pressure, psia

RDP	Relative dynamic parameter
Re_∞	Free-stream unit Reynolds number, 1/ft
S	Parachute reference area, $in.^2$; for 5-in.-diam canopy, S = 19.635 $in.^2$; for 8-in.-diam canopy, S = 50.265 $in.^2$
T_o	Free-stream stagnation temperature, °R
T_T	Measured probe temperature, °R
X/D	Probe position in axial direction divided by forebody cone base diameter (6 in.)
Y/D	Probe position in lateral direction divided by forebody cone base diameter (6 in.)
Z/D	Probe position in vertical direction divided by forebody cone base diameter (6 in.)
Z_1, Z_2	Parameters derived from skewness and kurtosis values